DOE/BC/96001243
(DE96001243)

EXPERIMENTAL TRACKING OF THE EVOLUTION OF FOAM IN POROUS MEDIA

Manuscript

By
David Cohen, T.W. Patzek, and C.J. Radke

July 1996

University of California, Berkeley
Berkeley, California

Bartlesville Project Office
U. S. DEPARTMENT OF ENERGY
Bartlesville, Oklahoma

DOE/BC/96001243
Distribution Category UC-122

Experimental Tracking of the Evolution of Foam in Porous Media

Manuscript

By
David Cohen
T.W. Patzek
C.J. Radke

July 1996

Prepared for
U.S. Department of Energy
Assistant Secretary for Fossil Energy

Tom Reid, Project Manager
Bartlesville Project Office
P.O. Box 1398
Bartlesville, OK 74005

Prepared by
University of California, Berkeley
Berkeley, California 94720-1462

Experimental Tracking of the Evolution of Foam in Porous Media

David Cohen,[1] T.W. Patzek, [2]and C.J. Radke[1]
Lawrence Berkeley National Laboratory, [1]Department of Chemical Engineering, and
[2]Department of Materials Science and Mineral Engineering, University of California,
Berkeley, CA 94720

Introduction

The mechanism of foam decay as a result of gas diffusion between adjacent bubbles results in the complete destruction of bulk foam. Gas diffuses from smaller bubbles to larger ones; as a result, the larger bubbles grow until there is only one large bubble remaining. Due to gravity segregation, the single largest bubble is on top of the foam. As a result, one can measure the pressure of this headspace and see how it changes with time as a result of gas diffusion. Nishioka and Ross[1] used this procedure to track experimentally the decay of bulk foam, by inserting a pressure transducer at the top of a closed container of bulk foam. The change in pressure corresponds to a change in bulk foam surface area following the Equation of State for Foam.[2]

Foam is generated in a porous medium is more complicated. Diffusion does result in redistribution of gas in foam in porous media, but does not ultimately collapse as a result of diffusion. Instead, foam approaches an equilibrium configuration, in which all the lamellae sit at the pore throats, where they exhibit zero curvature.[3]

The bubble pressures in a foam in a porous medium change as the foam undergoes diffusion-driven coarsening. However, the nature of such a system makes it nearly impossible to do a simple measurement such as the one described above for bulk foam. Local gravity segregation does not occur in systems with low Bond number. Each pore body acts as a large bubble surrounded by a number of higher pressure bubbles which span the pore throats. Current technology does not allow one to localize a small transducer in a pore body to track the pressure in this space.

One solution to this problem is to create artificially a large bubble adjacent to the porous medium which acts as a "headspace." The idea for doing this is based on the work of Flumerfelt and Chen,[4] who used semi-permeable membranes on each side of a bead pack to separate the liquid and gas phases and thus ascertain the capillary pressure by measuring the difference in pressure between the phases. We present here an idea for measuring the capillary pressure at different positions along the length of a cell packed with a porous material. On each side of the core are openings that can be covered with the same semi-permeable membranes used by Flumerfelt and Chen. When a membrane which is impermeable to the liquid phase is placed in one of these openings, the other side of this membrane acts as a gas headspace, which is significantly larger than any of the pore bodies. Attaching a transducer to this opening allows us to measure the change in gas phase pressure in this headspace as a result of diffusion.

Just as in bulk foam, the pressure in an artificial headspace adjacent to a porous medium accepts gas from around it as a result of diffusion. If we were able to generate a foam in the porous medium which on average had uniform pressure, but had some distribution of bubble sizes, we would see an increase in the pressure of this headspace. However, as we will see, the process of generating foam in a porous medium results in a significant pressure drop in the direction of foam flow. The presence of this gradient in pressure interferes with our ability to measure accurately the increase of pressure in the headspace.

It is very hard to create a foam which is devoid of the effects of multiphase flow through a low permeability porous medium. Foam is generated *in situ* by mechanisms of snap off, lamella division, and lamella leave-behind.[5, 6] As more and more lamellae are formed by these mechanisms, the foam texture, or number of bubbles per unit volume, increases. As this happens, the pressure required to push the foam through the porous medium and generate more lamellae increases.[7, 8] After a period of time, the pressure gradient approaches a steady state,[9] at which point the average texture is constant. This

does not mean that bubble generation and coalescence have stopped. Instead, this means the rate of formation of new lamellae is perfectly balanced by the rate of coalescence of existing lamellae.

If inlet flow is stopped and the foam is isolated at steady state flow, the foam undergoes a relaxation. It is during this time that two things occur. One is a continuation of hydrodynamic flow until the driving force is exhausted and the foam becomes stationary. The other is an equalization of gas pressure everywhere in the system as a result of gas diffusion from bubble to bubble. It is not until this latter process is complete that the pressure drop across a region of foam totally disappears. By tracking the pressure drop across a core filled with foam after foam generation is complete, we can therefore learn a great deal about the process of foam relaxation and the time scale for diffusion by simply measuring the pressure drop as a function of time.

We have explained that diffusion does not result in the total destruction of foam in a porous medium. On the other hand, the result is a stable foam with all the lamellae sitting at the pore throats. We cannot observe the individual lamellae in a three dimensional core in order to verify this conclusion. However, we do know that the pressure drop across the core goes to zero. In order for this to be true, the lamellae either have to coalesce or they must all obtain a position of zero curvature, such as they would at the pore throat. If the latter were true, then the core contains a strong foam even after the diffusion process has been given a significant period of time to complete, and a large pressure drop would be required to mobilize the equilibrium foam. By allowing the remaining fluid in the porous medium to simply drain out of the core and measuring the pressure drop that results, we show that the equilibrium configuration is a foam with uniform pressure.

In this paper, we discuss the experiments that have been done to track the effects of diffusion of gas in foams trapped in porous media. We describe several types of experiments and discuss the difficulties that prevent quantitative results from being

obtained in most cases. However, the experiments do help us understand the physics of diffusion-driven coarsening of foams trapped in porous media. This understanding is necessary to simulate the behavior of these foams and predict the mobilization characteristics of foam in porous media.[3,10] At the end of this paper, we compare the trends and predictions resulting from the experimental work to the predictions of the models which are presented elsewhere.

Experimental Apparatus

The apparatus consists of a core, liquid and gas delivery systems, and pressure measurement devices. The central part of the system is the core, which is packed with glass beads to act as a porous medium.

Porous Medium Core

A diagram of the core design is shown in Figure 1. A hollow region was cut out of a solid block of Plexiglas with a 4.6 cm square cross-section. The core can withstand up to 200 psig of pressure. The interior has a square cross-section with 2.6 cm sides. The main body is 10 cm long and has 3 pairs of opposing ports along its length. Each port is a threaded opening 2 cm in diameter. These ports can be capped or used as pressure taps.

The core is held together by four 12 1/2 inch screws which run through the corners of the main body and press three centimeter long stainless steel end caps in place. The first centimeter is square and the other two are circular. The circular region of each end cap has a 2.6 cm circular hole on the inside, into which fits a distributor plug. The distributor plug is held in place with a sleeve that screws onto the end cap. Figure 2 is a photograph of the empty core and stainless steel pieces held together by the screws.

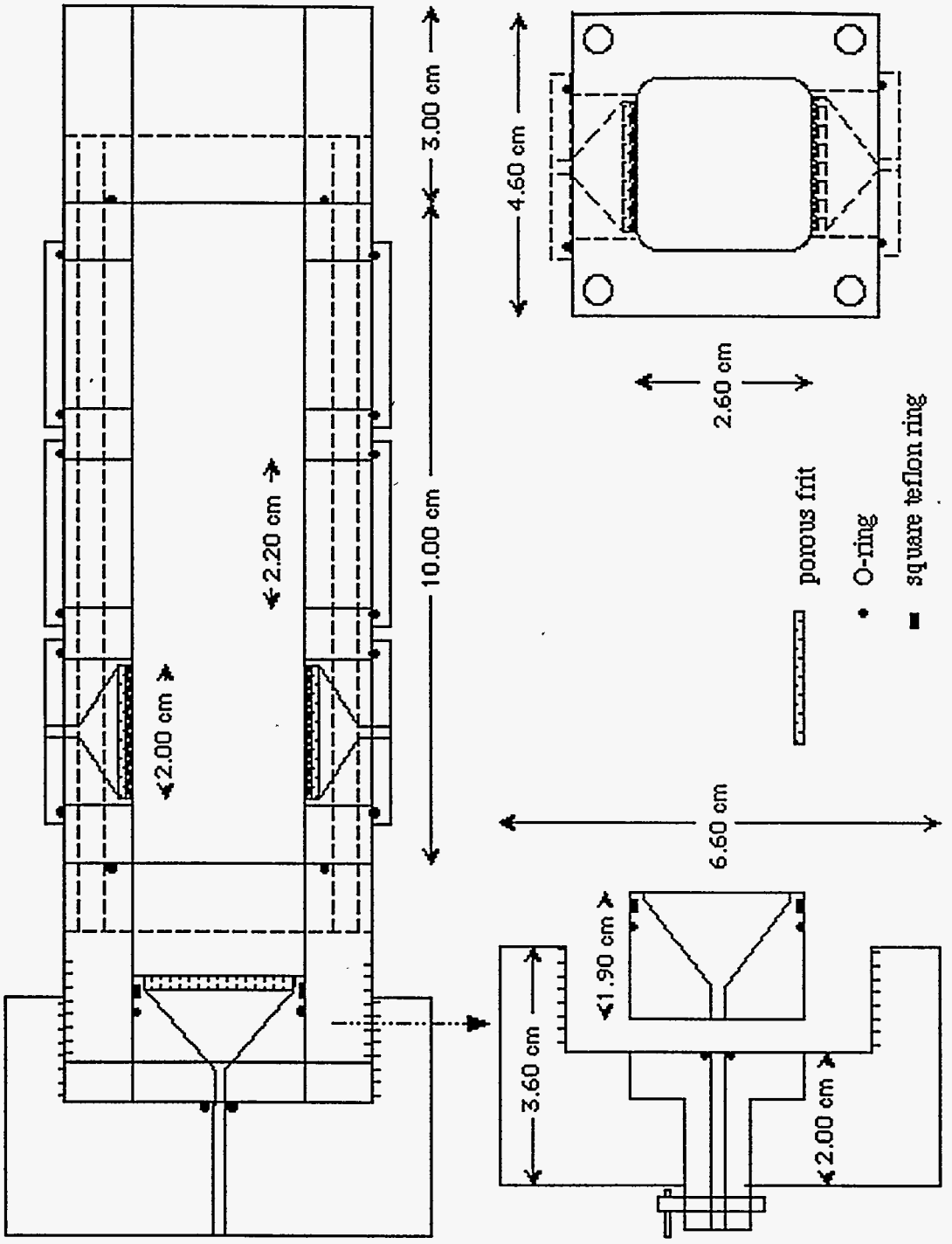

Figure 1: Design diagram for experimental core. Three drawings: side cross-section of core; detail of end cap and distribution cap; and end cross-section.

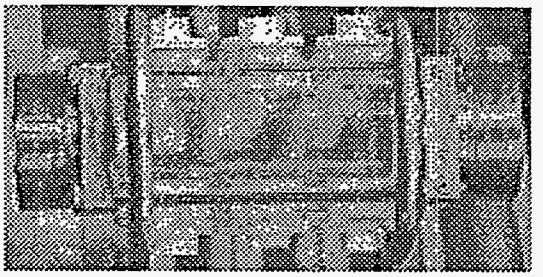

Figure 2: The Plexiglas core has stainless steel pieces on each end and the entire assembly is held together with screws that run through the corners of the core.

The distributor plug has a 1/16" opening on one side which funnels out in order to allow even distribution of flow over the full cross-section of the core. The end of the funnel has space for a frit or a support screen. Both of these are porous so that the fluids will flow through, but are there to hold and compress the small glass beads inside the core. The frits are Kontes porous-polyethylene discs (K-952100-0025). The support screens are cut from Type 316 Stainless Steel Support Screens from Gelman Sciences. The frits create more resistance to flow than the support screens, so sometimes it is beneficial to use one rather than the other.

The funnel end of the distributor plug has a square teflon ring on the outside. The ring has beveled edges on the outside and rubs against the inside of the bore to make sure that all the glass beads are pushed in as the plug is tightened into place. There is an O-ring just behind the teflon ring to complete the seal. Tightening the sleeves on both ends pushes the distributor plugs against the packing, thus creating a tightly packed porous medium.

There are two types of plugs which screw into the ports along the side of the core. They both are made of Viton and have the same basic shape. An O-ring fits at the top of the threaded part of the cap, which is 2.2 cm in diameter. The tops of the caps are 2.6 cm in diameter and have hexagonal protrusions that allow the plugs to be turned using a wrench. One type of plug is solid all the way through and is put in place just to seal off the side of the core.

The second type of plug is a pressure tap. The design of a pressure tap is shown in Figure 3. The bottom of the tap has a place to insert a semi-permeable membrane resting on a support screen. Above this is a tapered funnel which narrows to a 1/16" opening. Above this narrow opening is a wider area for attachment of tubing using Swagelok™ fittings. Pressure transducers can be connected to the pressure taps in this manner.

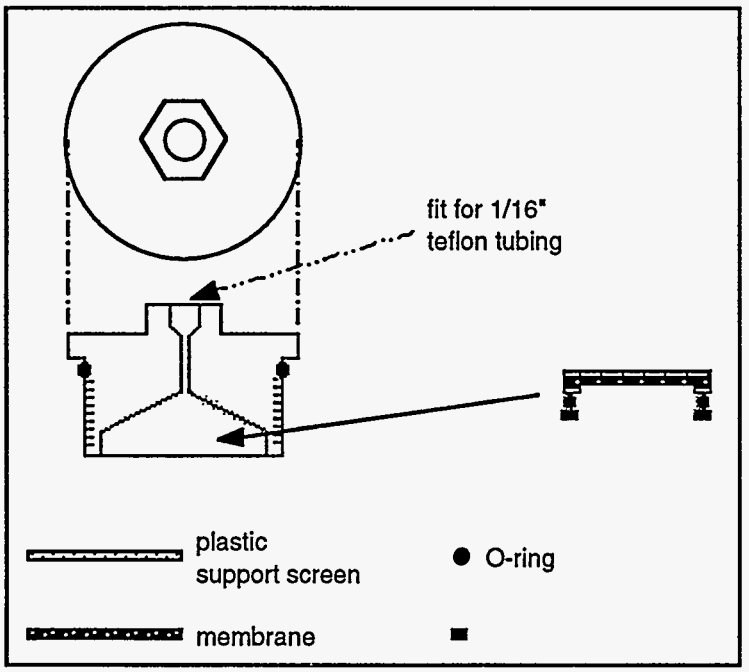

Figure 3: Pressure tap plug design. On the right of the figure is an explanation of how the membranes are secured in place with a series of layers.

Small glass beads make up an unconsolidated, monodisperse porous medium. The beads are available in sizes from 45 μm to 1 mm in diameter. The 45 μm beads are Jencons UK Grade 18 beads. The 150 μm to 1 mm diameter beads are Microbeads from Cataphote. Beads of one size are packed into the core by the technique described later.

Phase Separation

When multiple phases coexist in the porous medium, it is sometimes desirable to measure just the gas pressure or liquid pressure in one of the caps. For this purpose, we have membranes from Gelman Sciences which are either hydrophilic, allowing just water phase to pass through, or hydrophobic, keeping liquid out. The hydrophilic membrane is a vinyl/acrylic copolymer, product number DM-450, with 0.45 micron pores. The hydrophobic membrane is polytetrafluoroethylene (PTFE), product number TF-450, also with 0.45 micron pores.

The membranes do a very good job of separating phases. In fact, the PTFE membrane was tested for integrity by pressurizing one side with water and it was found to withstand 40 psig without any breakthrough. However, the membrane must be installed in the pressure tap correctly, so that water does not pass around the edges. To do this, there are several layers that are installed, shown in Figure 2. First, a perforated plastic support screen must be snapped into place, and the membrane rests on this screen. The outer edge of the membrane is attached to a plastic ring by epoxy glue. An O-ring rests against this plastic ring and the whole assembly is held in place by a threaded ring, which is tightened using a specially designed wrench. If installed carefully, this entire assembly seals the edges of the membrane so that no liquid seeps around it as a result of capillary suction.

The apparatus can be used for several different types of measurements. One is the determination of gas pressure or liquid pressure adjacent to the porous medium. This type of measurement is carried out by using one of the pressure taps with a hydrophobic or hydrophilic membrane. Measuring the pressure difference between these two phases gives a "capillary pressure" similar to those measured by Flumerfelt and Chen[4] in 1990. They generated foam in a packed cell and then waited until the pressure equilibrated and took a "capillary pressure" measurement. The evolution of the pressures during the period of equilibration is what we are investigating in this study.

Rather than measure the pressure of both phases, we measure just the change in gas phase pressure during equilibration of the foam. The volume of gas on the far side of the PTFE membrane including the line connecting to the transducer acts as a "headspace" adjacent to porous medium. This headspace is analogous to the headspace pressure measured by Nishioka and Ross[11] and Monsalve and Schechter[12] for bulk foam. The design of the core allows for measurement of the pressure in a headspace at one of three locations along the core as the foam evolves due to diffusion. Since water is the continuous phase in foam, its pressure is not expected to change. Therefore, we decided not to measure the liquid phase pressure.

If a perforated screen is used in the pressure taps instead of a semi-permeable membrane, the foam pressure at a specific location in the porous medium is measured. The tap comes in contact with a large number of pores, so the pressure that is measured is an average pressure over a region of the porous medium.

The apparatus can also be used to measure the differential pressure between any pair of pressure taps in the core or between the two ends of the core. This can be done with two pressure transducers or with a differential pressure transducer connecting two locations.

Pressure Measurement

To measure differential pressures along the length of the core, a Validyne KP15 transducer is used. This transducer has exchangeable stainless steel plates that are sensitive to different pressure ranges. After installing the proper plate, the transducer must be calibrated. After this is done, the transducer is installed between two pressure taps of the core to measure the pressure difference. The core is shown in Figure 4 with the Validyne transducer in place. The output from the Validyne transducer is sent to a strip-chart recorder.

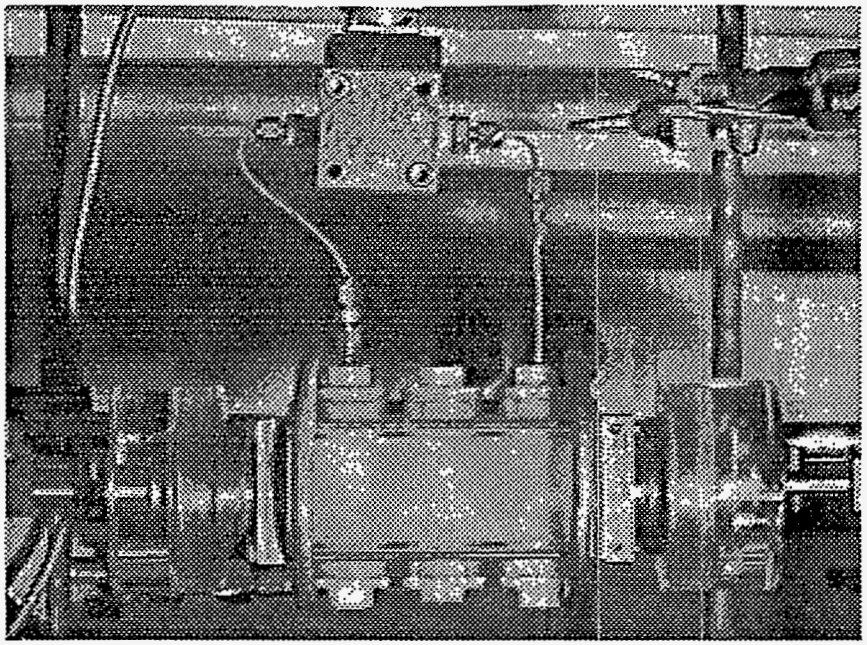

Figure 4: Picture of the experimental core packed with glass beads. The Validyne KP15 pressure transducer is in position to measure the pressure difference between the first and third pressure taps along the core.

Other pressure measurements are taken using Druck PDCR 22 transducers, which use single crystal silicon diaphragms to measure low differential pressures between any medium and a gas. We usually use the PDCR 22 to measure the pressure differential between the medium and the air in the room. The PDCR 22 transducers are calibrated to differential pressures of 1, 2.5, and 5 psig. The transducer is connected to the tubing using a Zero Volume Pressure Adapter (ZVPA) from Scanivalve Corporation. The ZVPA allows the face of the transducer to be mounted very close to the medium being measured and has a bleed valve to purge air out of liquid filled lines or to zero the transducer. Care must be taken not to over pressurize the PDCR 22 transducers, as they are very easily damaged.

A Druck PDCR 820 transducer with a range of 0-200 psi is used to measure input pressure to the core. Like the PDCR 22, the negative side of all the PDCR 820 is for gas service only, so it must not come in contact with liquid.

The Druck transducers are read by a seven channel DPI 420 indicator with IEEE interface. The output from the indicator connects to an IEEE card in a Macintosh IIci computer. The computer is equipped with LabView 2 software and an instrument driver was written to read the pressures from one to three channels at time increments selected by the user.[3]

Entire Apparatus

The flow sheet for the entire apparatus is shown in Figure 5. Foam is generated by mixing surfactant solution with nitrogen gas in the bead pack porous medium. The surfactant solution is pumped at constant volumetric flowrate using an ISCO Model 100D Syringe pump. The pump accurately delivers a constant flowrate of surfactant at any system pressure. It is accurate down to very low flowrates, as low as 1 microliter per minute. The nitrogen is also introduced at constant volumetric flowrate, using a Brooks 5850 Mass Flow Controller. The gas to liquid flow ratio we use is usually 10 to 1, but good results may be achieved with a higher ratio. The nitrogen and surfactant flow together at a "T" in the line and then into the packed core, where foam is generated *in situ.* The downstream end of the core drains into a beaker. The amount of displaced fluid can be measured at the outlet, then the output can be simply discarded.

The Druck 820 pressure transducer is located on the upstream side of the core to measure the inlet pressure to the core. There is also a pressure relief valve calibrated to 200 psi, which protects the core from over pressurization. The core is surrounded by a pair of valves which, when closed, isolate it. In this manner, stationary foam remains trapped inside the porous medium and the evolution of its pressures can be tracked. Inside this set of valves, we can measure the differential pressure with a Validyne transducer connected to a strip chart recorder, or by using Druck transducers to measure the pressures at two different taps and then calculating the difference.

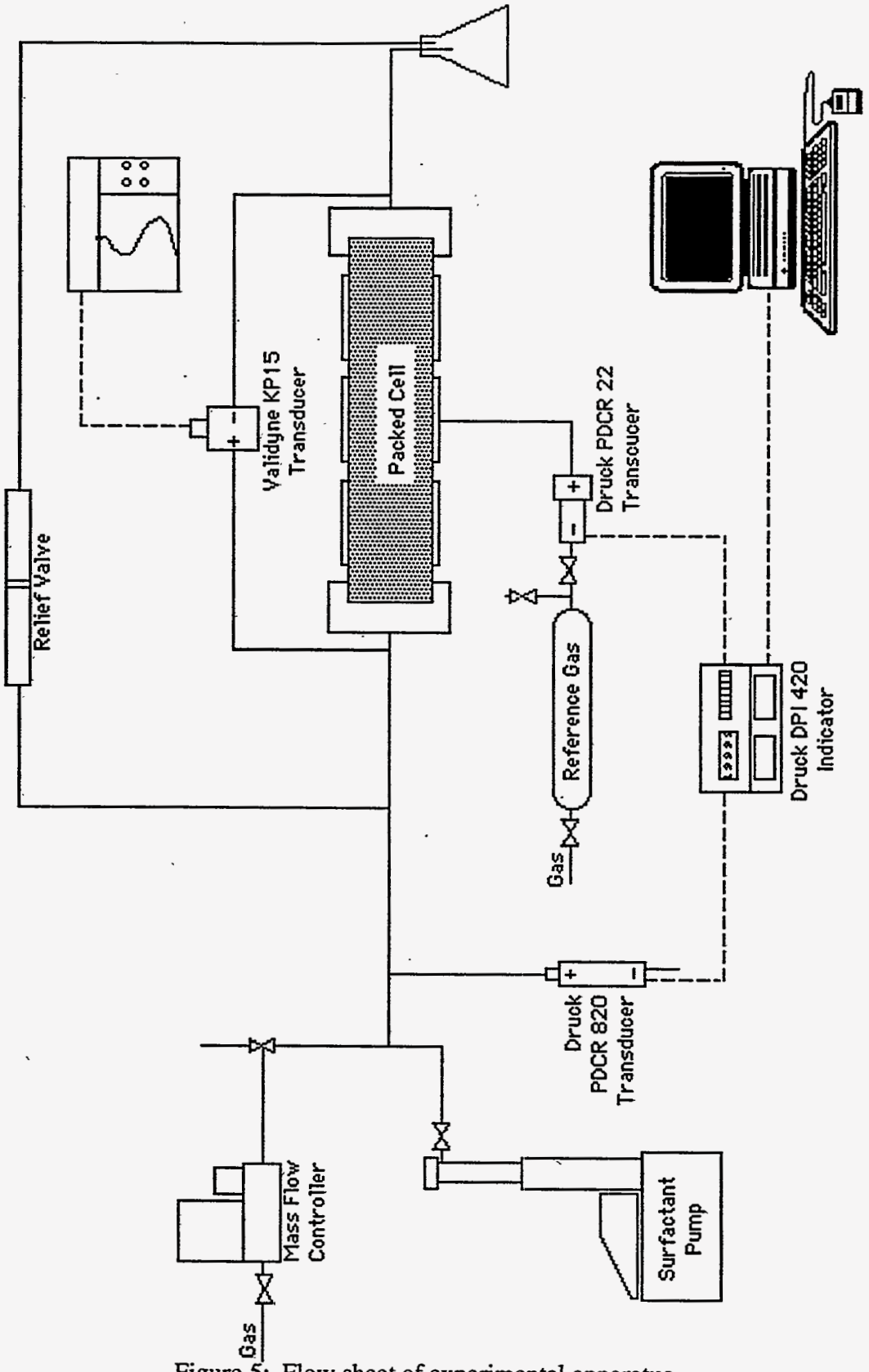

Figure 5: Flow sheet of experimental apparatus.

Figure 5 shows a Druck PDCR 22 transducer connected to a central pressure tap on the core. In the figure, the transducer is also connected to a reference volume. The reference volume is sometimes necessary to make sure the differential pressure across the transducer does not exceed its operating range. As the pressure on the positive side of the transducer grows, gas is released from the tank to the negative side of the transducer through a needle valve. This correction is not necessary for the larger bead packs, as the absolute pressure in the porous medium remains within the transducer's range. But for the 45 μm beads, the absolute pressure in the core can exceed 100 psia, and the reference side of the transducer needs to be pressurized.

The location of the transducer in Figure 5 is one of six possible locations along the core. In addition, there may be several transducers attached at one time. The signals from the Druck transducers are connected to the DPI 420 pressure indicator, which communicates with a Macintosh IIci computer.

This apparatus allows tracking of the differential pressure and also gas and liquid pressures at different locations along the core during flow and after flow has been stopped. In addition, the differential pressure can be measured as foam drains out of the core. The flow rates are adjusted using the mass flow controller and ISCO pump. This allows for the generation of foams of different qualities.

Experimental Procedure

Before an experimental run, the core must be properly prepared. It is disassembled by unscrewing the end sleeves and pulling out the distribution plugs. The end and transducer caps and the interior of the core are rinsed with deionized water and the threads are cleared of residual glass beads. For the particular experimental plan, a custom cap configuration is used. Any combination of cap choices may be used; the possible caps are plugs, pressure taps with no membranes, or pressure taps with

hydrophilic or hydrophobic membranes. Before the core is packed with beads, the cap configuration of choice is installed along the length of the core.

A fresh bead pack is used for each experiment. With one distributor plug and sleeve in place, the core is filled with the desired glass beads. The beads are kept wet with deionized water while packing them into the core. As the beads are poured in, it is important to make sure they are uniformly packed, clearing out air pockets which form by reaching into the cell with a scoop and swirling it around. When the core is nearly full, the second distributor plug is inserted and the sleeve is screwed on. The two sleeves are hand tightened to compress the beads so as to create a nearly uniform, tight packing.

After the core is completely assembled, it is put in place in the apparatus, as in Figure 5. Transducers are attached as necessary to the inlet side of the core and to the pressure taps, using Swagelok™ fittings. Most of the tubing and fittings are 1/16". Care must be taken not to over tighten the Swagelok™ fittings. The tubing is put together initially using a steel tightening accessory from Swagelok™. Subsequently, each time the fittings are tightened it requires less than one quarter turn with a wrench to seal adequately. Tightening too much may damage the ferrules and result in a leaky system.

Once the core is in place, it must be saturated with aqueous surfactant solution. The surfactant solution used in the experiments is a 0.5 weight percent solution of sodium dodecyl sulfate (SDS). The solution is made from electrophoresis grade sodium dodecyl sulfate from Kodak. The concentration used is a little more than twice the critical micelle concentration (CMC) of 2.34 g/l. The ISCO pump is filled with the solution and then used to pump the surfactant solution through the core. This is usually done with a flowrate of 1 ml/min for about an hour. When packed with spherical beads, the core has a void fraction of 0.35. The core has a total volume of about 95 cm^3, so the pore volume of the porous medium is just over 33 cm^3.

The raw materials for foam generation are the surfactant solution and nitrogen gas, supplied from a high-pressure gas cylinder. We use a total flow rate of nitrogen and

surfactant of 2.2 cm^3/min. This is equivalent to a Darcy velocity of 15.45 ft/day. Using a gas to liquid flow ratio of 10 to 1, the flow rate of nitrogen is 2 ml/min, while that of SDS solution is 0.2 ml/min. These flow rates were used in all subsequent experiments described here.

The gas cylinder is opened to pressurize the upstream side of the mass flow controller. The pressure differential across the mass flow controller must lie between 10 and 50 psi, so as the pressure in the system increases, the upstream pressure to the mass flow controller must be appropriately adjusted. The full range of the mass flow controller is 10 cm^3/min, so it should be set at 20% in order to produce 2 cm^3/min nitrogen flow. There is a three-way valve on the downstream side of the mass flow controller which is used to "turn on" the nitrogen flow to the system or quickly stop nitrogen flow to the system. If the three-way valve is not directing flow towards the inlet of the core, it vents the nitrogen to the atmosphere. When venting to the atmosphere, care must be taken that the pressure difference across the MFC does not to exceed 50 psi.

The SDS solution is delivered by the ISCO syringe pump. The pump delivers low flow rates accurately up to 10,000 psi. A maximum pressure limit can be programmed into the pump controller so that the pressure out of the pump does not get dangerously high. The core is designed to withstand 200 psi, but to be safe, we do not want to approach that value. For this reason, we also have an in-line relief valve which vents at 200 psi.

As foam is generated, the pressure difference across the core builds. Depending on the permeability of the porous medium, the pressure required to push foam through a 10 cm core can be well above 100 psi. The permeability of a porous medium packed with spherical beads is calculated using

$$K = cR^2 \qquad [1]$$

where R is the diameter of the beads and c is a constant, which for spheres is $6x10^{-4}$.[13] When the column is packed with 1 mm glass beads, the permeability is 152 μm^2, or 152 Darcy. The maximum pressure gradient achieved by foam in this case is below 5 psi. On the other hand, the 45 μm glass beads, permeability 0.31 Darcy, require 100-200 psi to flow a well developed foam through them. The magnitude of the gradient can be affected by the presence of a fritted disk at the end of the distributor plug. These fritted disks support a significant pressure gradient across them, so it is difficult to separate the effect of foam flow through the fritted disk from foam flow through the bead pack. For this reason, we use stainless steel support screens which are thinner and more permeable.

If one of the PDCR 22 transducers is being used to measure pressure alongside the core during a run where the absolute pressure is above the calibrated operating range of the transducer, it is necessary to use the reference side gas volume to keep the differential pressure down. To use the reference side gas volume, we fill it initially with nitrogen gas to between 50 and 75 psi nitrogen. Then, as the pressure on the positive side of the PDCR 22 transducer increases, the negative side is pressurized by bleeding gas through the needle valve. There is also a needle valve that allows the system to go in reverse by bleeding the nitrogen from the negative side of the transducer to the room.

The 1/16" lines on the downstream side of the ISCO pump and the mass flow controller join together at a tee, where the gas and liquid mix and flow together into the packed core. Foam is generated *in situ* in the core by mechanisms of snap-off, lamella division, and lamella leave behind.[5, 6, 14, 15] As foam is generated in the core, the surfactant solution which was in the porous medium at the beginning is displaced out the downstream end. After a period of time, foam begins to emerge out of the core. The foam generation process continues until steady state has been reached.

Steady state is reached when the pressure drop across the core no longer changes and the foam quality at the downstream end of the core is constant. The pressure drop often oscillates quite a bit, so we wait until it deviates around a nearly uniform value.

Previous studies have found that it takes as much as 12 pore volumes (PV) to reach steady state in somewhat similar length beadpacks.[9] When our core is packed with 0.25 mm beads, we have seen steady state achieved after 5 PV. Figure 6 shows a plot of pressure drop across the cell as a function of PV injected.

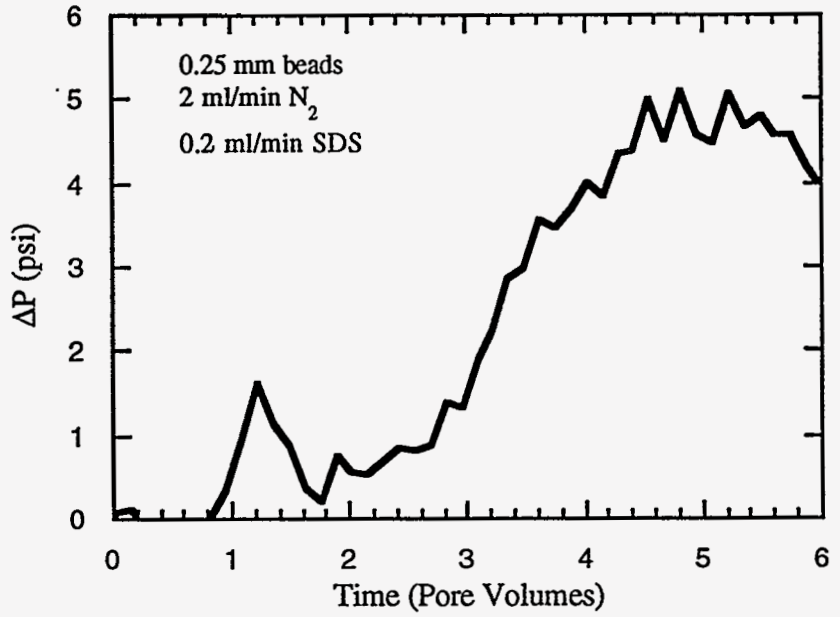

Figure 6: Pressure drop across core packed with 0.25 mm beads as a function of pore volumes (PV) injected. Steady state is reached after 5 PV have been injected. In this experiment, flow was stopped at 5.5 PV, and the ΔP began to decrease.

When steady state is reached, the valves on either side of the cell are closed to isolate the foam in the cell. Very quickly, the ISCO pump must be shut off and the three way valve on the downstream side of the mass flow controller must be turned towards the atmosphere. After isolating the mass flow controller from the cylinder, the cylinder must be closed off and gas is allowed to drain from the gas lines. Care must be taken not to create a back-flow through the mass flow controller. Finally, the mass flow controller setting should be moved to 0%.

The quality of foam in the core is the volume fraction of gas flowing into the cell.[16] A good dry foam should have a quality of at least 90%. The foam quality in our experiments is approximately 91%.

Gas saturation is the fraction of the void volume which contains gas. Measuring the gas saturation is done by collecting and measuring the amount of liquid that comes out of the column during foam generation. The volume of the pore space in the packed cell, assuming a void fraction of 0.35, is 33 cm^3. So the amount of liquid remaining in the cell after foam generation can be calculated by adding together the void volume and the total liquid inflow, which is the flow rate times the duration of flow, and by subtracting from that sum the amount of liquid collected at the outlet of the cell. The gas saturation is the difference between the void volume and the liquid content, divided by the void volume.

In order to ensure that we see primarily pore effects, it is important that the Bond number (Bo), which compares the magnitude of the gravity forces to that of the capillary forces, be small. A Bond number of 1 indicates that the partitioning of two phases in a porous medium is equally dependent on gravity as it is on capillarity. The Bond number is defined as

$$Bo = \Delta\rho \, g \, h / (2 \, \sigma / r) , \qquad [2]$$

where $\Delta\rho$ is the density difference between the phases, h is the height of the region, σ is the surface tension of gas-liquid interface, r is the radius of the pore throat, and g is the gravitational constant.

Figure 7 shows the Bond number as a function of bead diameter in our packed bed porous medium, with a height of 2.6 cm. For this calculation, the pore throat radius is defined as 20% of the bead diameter. For all the beads used in this study, up to 1 mm, capillary forces are more important than gravity forces. However, for 1 mm diameter

beads, the Bond number is 0.73, so ignoring gravity may not be a good approximation. Beads which are 0.25 mm or smaller do allow this approximation to be made with confidence.

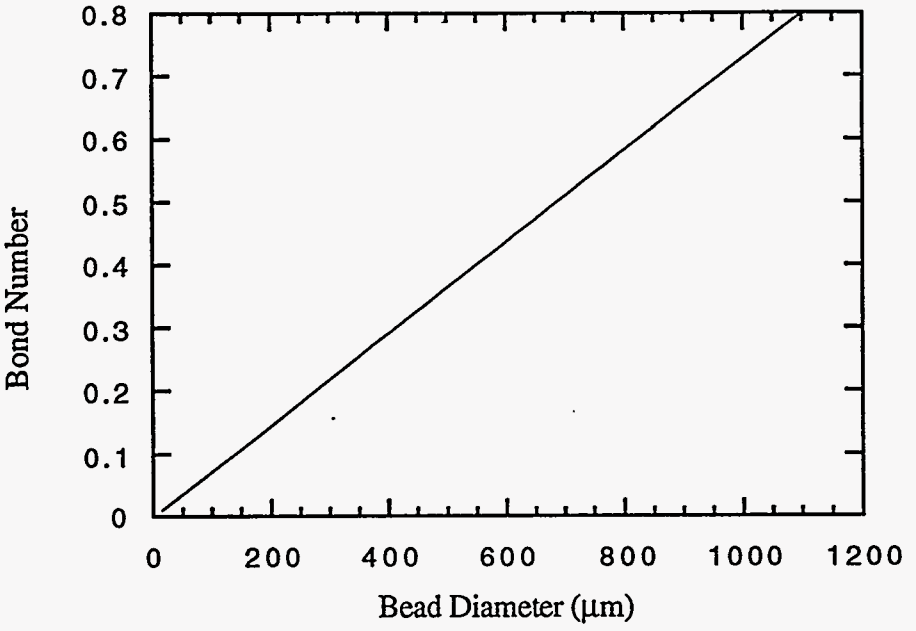

Figure 7: The Bond number of water-gas systems in a porous medium is a function of the size of the pore spaces, and thus a function of the diameter of the beads used as the packing.

With a well-developed foam isolated in the packed core, we are ready to measure the behavior of stationary foam in a porous medium. The first type of measurement which may be done is the observation of the pressure of a single phase of the foam during the process of relaxation to equilibrium. The particular phase whose pressure is to be measured is separated from the other by one of the membranes described earlier. The second type of measurement is the evolution of the pressure difference across the core. This can be done between any pair of points. Most often, the pressure difference is measured either between the two outside ends of the core or between the first and third pressure ports of the core. The pressure difference can be measured with no membranes in the line, or the gas pressure difference can be measured with PTFE membranes in

place. It may take several days for the pressure difference to relax completely, so the experiment often takes an entire week from beginning to end.

When the investigation of the stationary foam is complete, the downstream valve of the core is opened to allow the foam to exit from the core. As foam emerges from the core, a new pressure difference develops and evolves. The evolution of this pressure difference can be tracked in the same manner as above.

Foam Generation

Foam was generated using the procedure described above. During foam generation, it was possible to observe the process by following the change in pressure drop as a function of time, as shown in Figure 6. Even more interesting is the ability to track the progress of foam generation by watching the location of the foam front through the clear sides of the core.

Due to the low mobility of foam relative to the flow of gas through a porous medium, foam tends to move as a piston, uniformly pushing its way through the entire porous medium. Locally, fingering occurs, but the main front is never too far behind the leading edge of the fingers. Looking through the clear sides of a core, it is not obvious that the location of the visible front represents the location of the front deep inside the core. However, Hanssen and Haugum investigated the relationship and found that observing the front through the walls of a core is a good indication of the location of the foam front throughout the porous medium.[8]

Before foam generation begins, the core is saturated with aqueous surfactant solution. As gas invades and foam forms, liquid is pushed out of the pores in a fairly uniform manner because all the pores are nearly the same size in a monodisperse bead pack. The visible color of the porous medium changes slightly as the phase in the pores changes from liquid to predominantly gas. The gas filled pores look brighter than the liquid filled pores. In this manner, it is easy to tell how far into the porous medium the

foam has invaded just by looking at the side of the core. Figure 8 shows a sequence of snapshots of the experimental core taken during foam generation, showing how the foam front progresses. Flow was from right to left during this experiment. The core was packed with 0.25 mm glass beads and the gas to liquid flow ratio was 10:1.

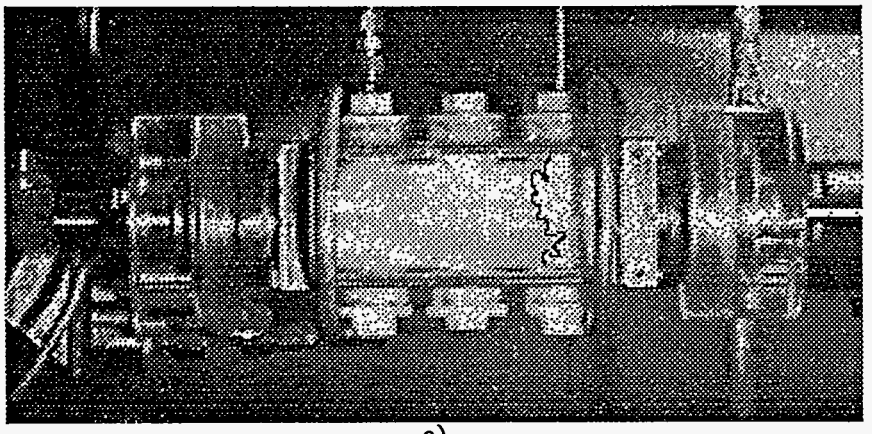

a)

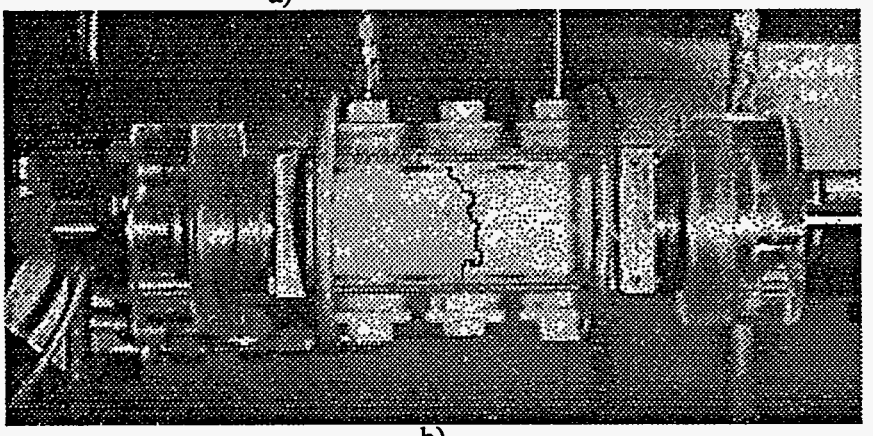

b)

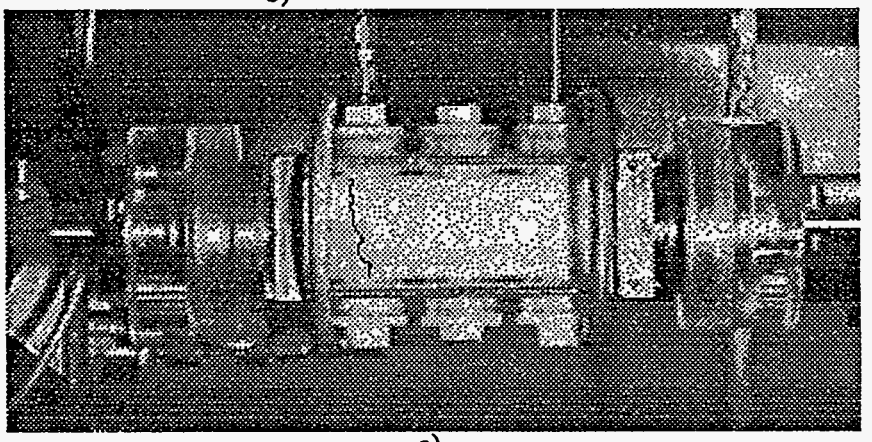

c)

Figure 8: A sequence of snapshots of during foam generation in the core packed with 0.25 mm beads. Flow is from right to left. The location of the foam front at each time is enhanced with a darker line.

Once the foam front reaches the left end of the core, foam breakthrough occurs. This is when liquid is no longer the only phase flowing out of the core. Foam is also flowing out. At this point, foam generation has not yet reached steady state. Foam texture continues to evolve and the pressure drop continues to increase for a period of time after foam breakthrough. Eventually, the foam flowing out of the cell has a very fine texture. Figure 9 shows strong foam flowing out of the core and filling a beaker. The white color of the foam indicates its high gas content and the small bubble sizes in the foam flowing out of the cell. The foam is stable enough to build up in the collection vessel as shown in the figure. The foam was collected in the beaker in Figure 9 over a period of about half an hour. Earlier in the foam generation process, weaker foams emerge and quickly break, but the steady state foam remains for several hours, even in a beaker open to the room.

Figure 9: Foam flowing out of the core at steady state. The bubbles are very small, the foam is stable, and it collects in the beaker.

Tracking Headspace Pressure

Bulk Foam

Nishioka and Ross published the first studies utilizing the equation of state for foam to measure the surface area reduction as a function of time in bulk foam.[1, 10] They

did this by measuring the pressure of gas external to the foam, in the headspace. In a closed volume, the headspace above a bulk foam grows and its pressure increases as the foam decays. This is because gas diffuses from the smaller bubbles in the foam into the larger bubbles, eventually moving into the headspace. Monsalve and Schechter[11] performed further studies of bulk foam decay. They made foam from Witconate AOS solution and saw pressure increases in the headspace of 4 cm H_2O over 60 minutes.

Experiments were run to try to recreate the data of the above studies. Foam was made using sodium dodecyl sulfate (SDS) solution in the empty experimental cell. The foam was generated by turning the cell on its end, filling the bottom of the cell with surfactant solution, and bubbling nitrogen up through the solution. The only other opening from the cell is through the top, where a transducer was attached. In addition, there is a valve which opens to the atmosphere. The configuration of the apparatus is shown in Figure 10. While foam is being generated, the valve is open, so the foam equilibrates with atmospheric pressure. A fine foam builds up in the cell and after a period of time, the top and bottom valves are closed in order to isolate the foam in the cell. The pressure in the headspace above the foam is measured using the transducer, and over time, the pressure changes.

The results of two runs of this experiment are shown in Figures 11 and 12. The results are fairly repeatable. At time zero, the headspace pressure is atmospheric, since the valve is open to the atmosphere immediately prior to the measurements. Hence, the pressures reported here are gauge pressures. The orders of magnitude of the pressure increase and time scale are comparable to those found in previous studies. The system takes about 50 minutes to reach equilibrium in both cases, and the pressure increases a little more than 2 cm of water. The data are presented in pressure units of cm water, which was used by previous researchers, and also in psig, in order to compare the magnitudes to the results of our other experiments. The unsteadiness of the data,

especially in first data set, is due to changing temperature and pressure conditions in the room, which affects the reference side of the transducer.

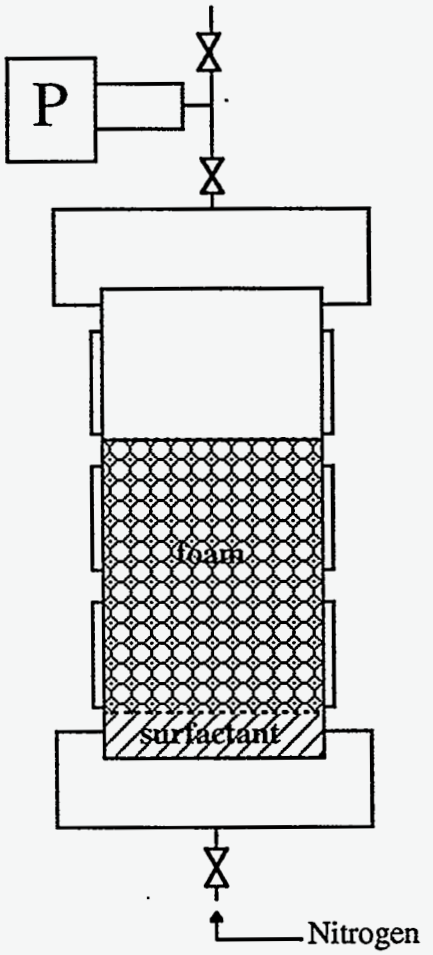

Figure 10: Using the cell to measure the headspace pressure change in bulk foam.

Monsalve and Schechter[12] and Patzek[17] showed that the evolution of foam surface area is sensitive to the initial bubble size distribution. Even foams that have the same initial surface area and volume will have different rates of area decrease as long as the initial bubble size distributions are different. This is the reason why reproducibility is very hard for foam experiments. No technique exists by which one can be sure that the initial conditions generated result in a specific initial configuration of bubbles.

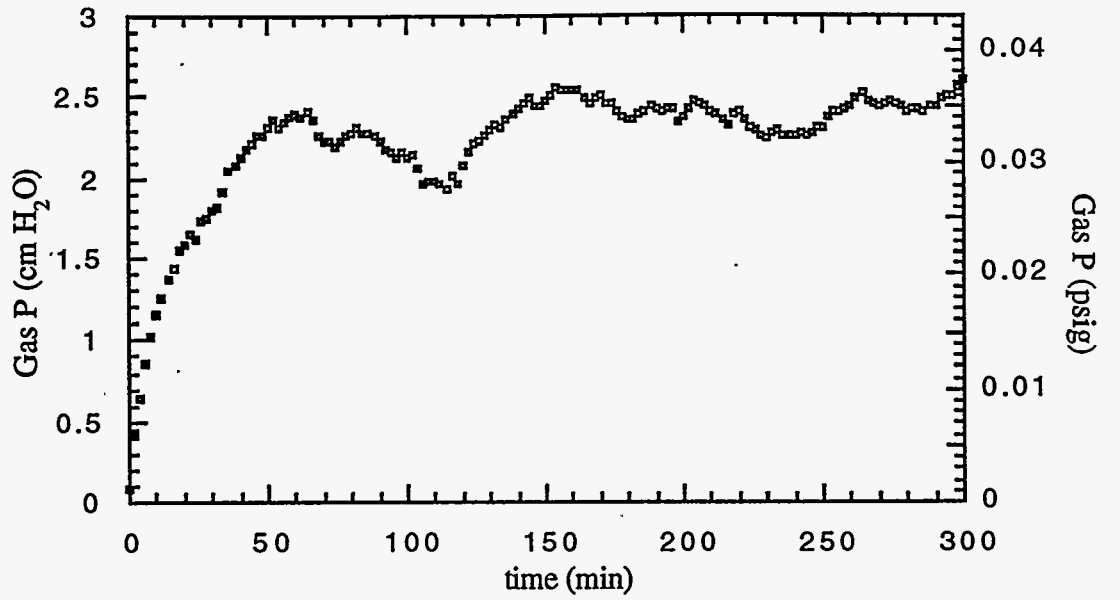

Figure 11: Bulk foam experiment. Plot of headspace pressure changing as a result of diffusion decay of SDS foam.

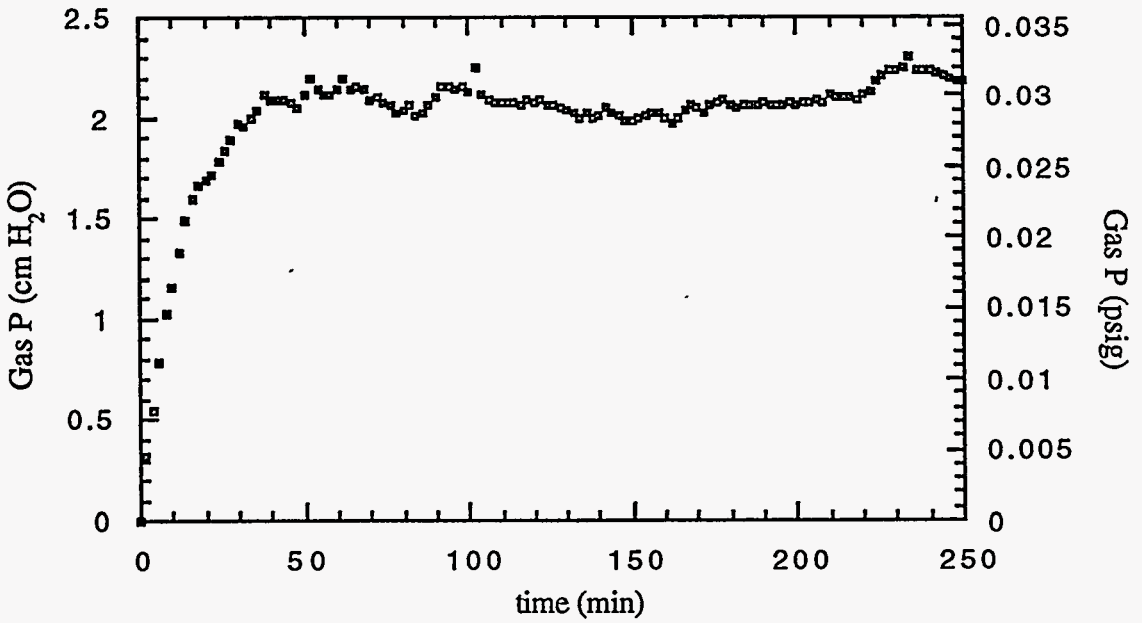

Figure 12: Additional SDS bulk foam experiment. Plot of headspace pressure versus time.

Foam in a Porous Medium

Foam in a porous medium exhibits behavior analogous to that of bulk foam. If there were a headspace volume adjacent to the region of the porous medium filled with foam, then its pressure would increase over time. But understanding what is meant by a headspace in this case is not trivial.

The pore space in a porous medium is made up of pore bodies and pore throats. Each pore body is connected to multiple pore throats. The number of throats attached to each pore body is called the coordination number of the porous medium. For example, Lin and Cohen[18] conducted a topological study of Berea sandstone and found that the coordination number typically ranges from 0 to 11, with an average coordination number of 4.

The bubbles which span a pore throat are at higher pressure that those which are in the pore body. An overly simplistic explanation is that bubbles in the pore throats are smaller than those in the pore body. Then the analogy can be made to bulk foam, where small bubbles are almost always at higher pressure than large bubbles. However, this explanation is fortuitous, because bubbles in a porous medium are constrained by the pore walls and therefore very often do not obey the rule of bulk foam, in which pressure inversely correlates to bubble size. A much better way to explain the pressure difference between the pore throat and the pore body is to look at the curvature of lamellae residing near pore throats.

The projection of a lamella in a water-wet pore intersects the pore wall at a 90° angle.[3, 5, 19] Because the walls of a pore slope towards the pore throat and because of the 90° angle of intersection, lamellae in physical equilibrium are always concave towards the pore throat. The Young-Laplace relationship demands that the pressure is higher on the concave side of a lamella. Thus, the pressure is always higher in the pore throat than in the adjacent pore body, as long as there is a lamella between the two.

A pore body can be thought of as a headspace since all the bubbles around it are at higher pressures. Gas diffuses out of the pore throats and into the pore bodies. Thus, the pressures in the pore bodies generally increase during the diffusion process. Cohen *et al.* presented simulations that verify this behavior.[10] Unfortunately, it is impossible to measure the pressure in an individual pore, so we cannot verify experimentally the above assertion.

On the other hand, it is possible to create an artificial headspace adjacent to the porous medium where we can measure the pressure and see if it increases as a result of diffusion. This is attempted using the pressure taps along the side of the experimental core. Each one of these caps has a diameter of 2 cm along its bottom face. Hence, a surface area of 12.6 cm^2 is in contact with a large number of pores which lie between the glass beads that make up the porous medium. When the cell is packed with 1 mm diameter beads, this means that over 40 beads come in contact with the bottom of the cap. The volume inside each cap is approximately 0.38 cm^3, several orders of magnitude greater than the volume of the pores in the bead pack. Hence this cap acts as a headspace analogous to the very large bubble on top of a container full of bulk foam.

Using the gas-only permeable PTFE membrane, the headspace pressure adjacent to SDS foams has been tracked. These are very difficult measurements for several reasons. First, and most importantly, when foam is generated in a porous medium, a significant pressure gradient along the length of the cell is established. When foam flow is stopped, diffusion begins. Diffusion is the mechanism by which the pressure gradient relaxes. This means that the gradient lingers for a while, during which time the pressures throughout the system are changing. It is impossible to separate this effect from the increasing headspace pressure. The pressure gradient can be minimized by using a bead pack with higher permeability. The highest permeability bead pack we can use and still have a Bond number less than unity is made up of 1 mm diameter beads. In this case, the overall pressure gradient created as foam flows through the system is under 4 psi.

Another reason these measurements are so difficult is that the magnitude of the pressure increase is very small. For this reason, it is necessary to use the highly accurate Druck PDCR 22 transducers to measure the increasing headspace pressure. Unfortunately, this problem is worse for the larger beads which are needed to minimize the pressure gradient. Larger beads result in lamellae that are less severely curved, and thus trap gas in the pore throats at a lower pressure. Consequently, the magnitude of the pressure increase due to release of gas from the pore throats to the pore bodies decreases as the bead size increases.

Nevertheless, it has been possible to obtain some data which show pressure increasing in the artificial headspace as a result of diffusion. One of these data sets is plotted in Figure 13. The system takes approximately 2 hours to reach equilibrium and the magnitude of the pressure increase is under 0.06 psi over this entire time. This is very similar to the magnitude of the pressure increase in the bulk foam experiments, where the headspace pressure increased by 0.03 psi during foam decay. Of course, the volumes of the headspaces in the two experiments are different, so the direct comparison of these magnitudes is not completely meaningful.

Successful experiments to show increasing headspace pressure for a variety of system conditions have not been achieved. There have been a couple of additional experiments in which the increase in headspace pressure was noticeable even though the pressure gradient relaxation dominated. Figure 14a shows the gas pressure at a pressure tap as a function of time for the core packed with 1 mm beads. The gas pressure increases as foam is generated between t=-90 and t=0 min, until a steady state is reached, at which point the gas pressure is just shy of 3.5 psig. At t=0, the inlet and outlet valves were closed, and the pressure immediately and quickly went through an adjustment. After 6 minutes of decrease, the gas pressure measured in the cap increased for about 120 minutes. Figure 14b gives a more detailed look at the change in gas pressure beginning from the isolation of foam in the core. The increase in pressure is due to the release of

encapsulated gas from the interior of the porous medium to the headspace adjacent to the core.

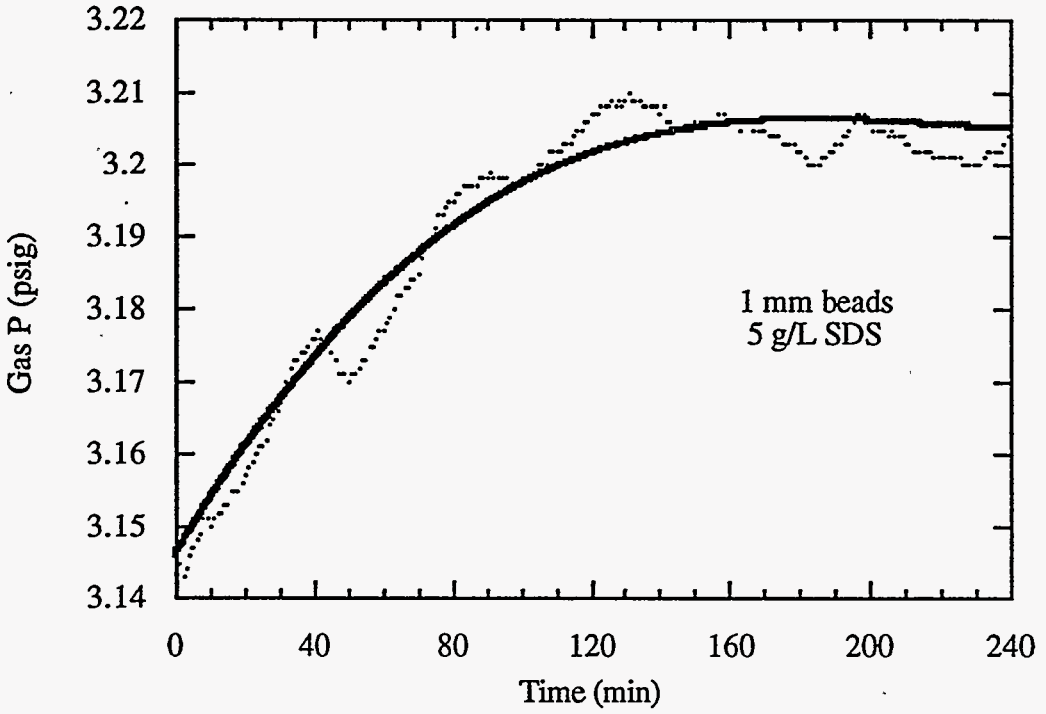

Figure 13: Experimental data showing the gas pressure increase in a headspace adjacent to a foam-filled core packed with 1 mm glass beads. The dots are the actual data, the solid line is a fit showing the trend of increasing pressure to a final equilibrium.

The experiment is hard to reproduce because it is impossible to generate the same initial conditions every time. For many experiments, the small increase in gas pressure is harder to resolve because the beginning of the increase blends into the end of the pressure adjustment. There were a number of experiments in which there was an obvious increase in gas pressure after the initial adjustment. But the fact that the pressure gradient which formed during foam generation undergoes relaxation and that the increase in pressure is very small makes it hard to rely on the experiment for quantitative conclusions.

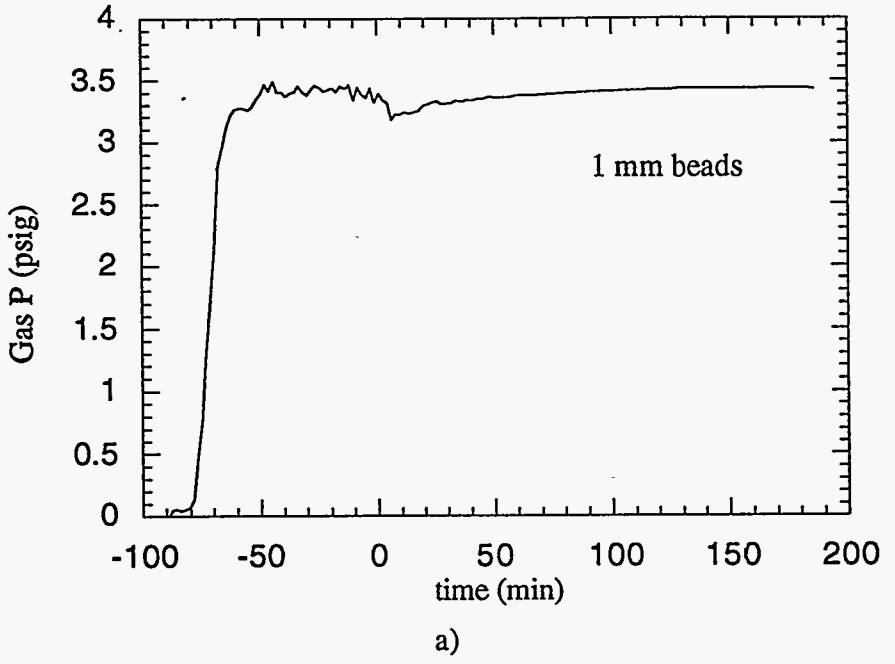

a)

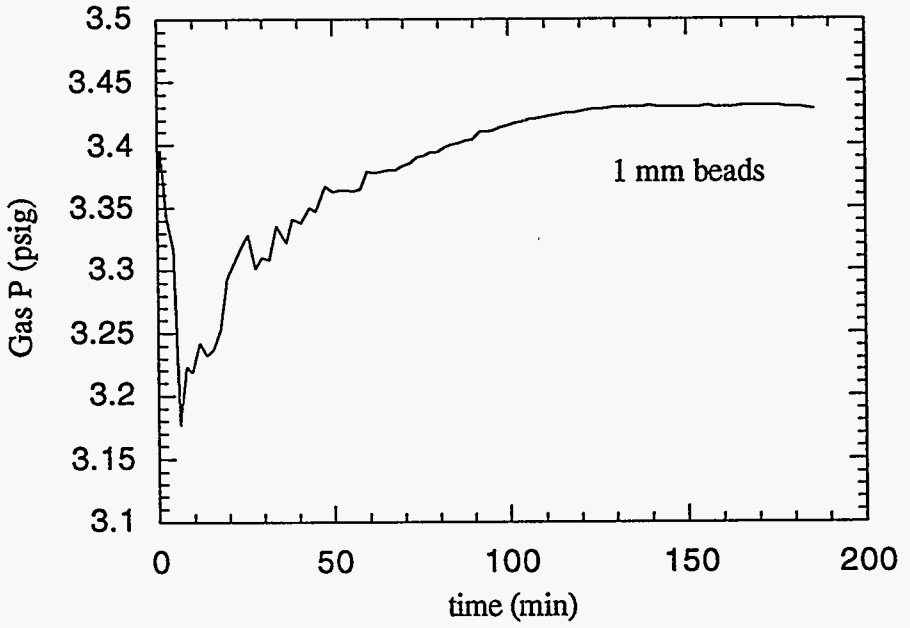

b)

Figure 14: a) Foam generation in 1 mm bead pack. Before time t=0, gas and SDS solution are flowing through the porous medium and the pressure at the central tap increases to steady state. b) At time t=0, flow is abruptly stopped. The pressure decreases first and then increases to equilibrium as a result of diffusion of gas to the headspace.

Pressure Drop Relaxation

The measurement of "headspace" pressure as a function of time adjacent to foam in a porous medium was successful for systems when the core was packed with large beads, specifically 1 mm in diameter. For smaller bead sizes, the pressure drop across the core is large and its relaxation process masks any increase in headspace pressure that occurs. But it is interesting to observe the evolution of the pressure drop as a way of understanding the system's approach to equilibrium. It is only when the pressure drop relaxes completely that diffusion stops.

Figure 15 shows the evolution of the pressure drop between the first and third pressure taps of the core. In this case, the core is packed with 500 μm diameter glass beads. The left side of the plot, at time t=0, represents the time at which the flow of surfactant solution and nitrogen gas through the core were stopped. Thus, at this point foam generation has ceased. It can easily be seen that the diffusion process lingers for a significant period of time.

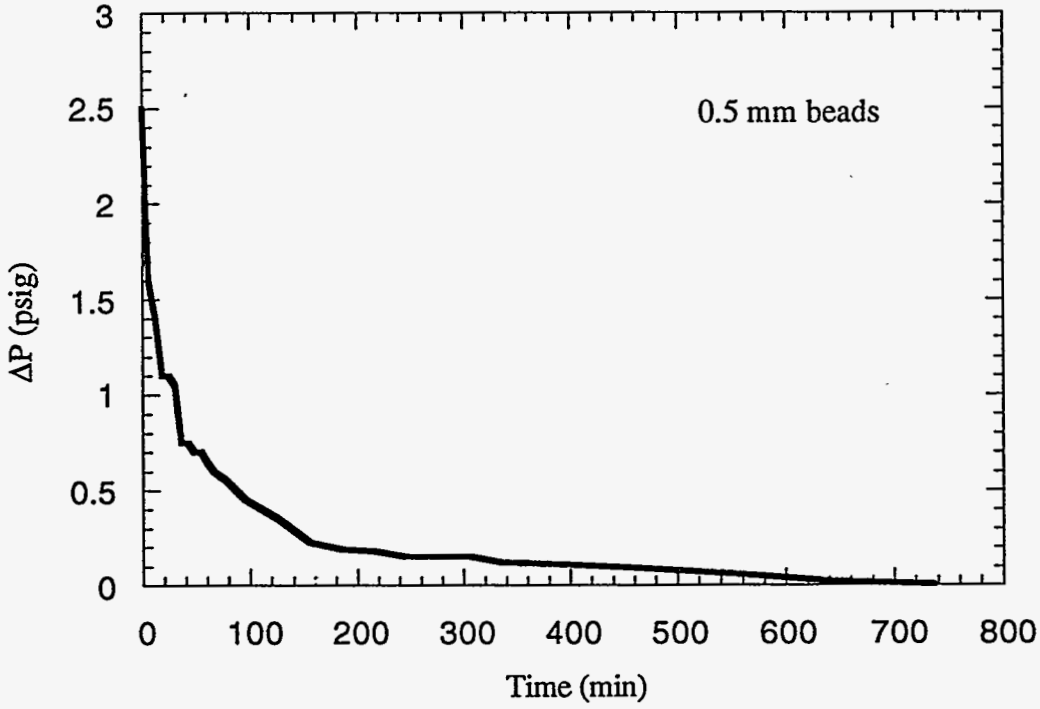

Figure 15: Pressure difference as a function of time between pressure taps 1 and 3 of the core packed with 500 μm beads.

As the permeability is reduced by using smaller beads, the initial value of the pressure drop increases, and the length of time it takes to reach equilibrium increases. It takes longer because the initial pressure drop is higher and more gas must be transferred by diffusion. Another reason it takes longer is that it takes more of the smaller beads to fill the same length of core. Therefore, the gas must diffuse through more pore throats and presumably through more lamellae to get from the high pressure side to the low pressure side. Figure 16 shows the results for a system with 250 μm diameter glass beads. The trends that are described above are easily verified by comparing Figures 15 and 16.

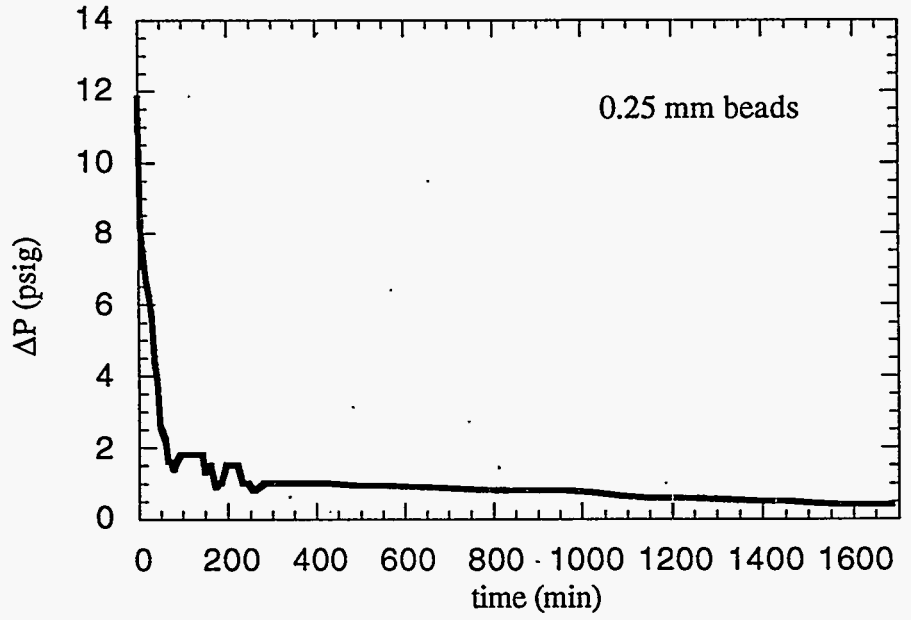

Figure 16: Pressure difference as a function of time between pressure taps 1 and 3 of the core packed with 250 μm beads.

Additional experiments were done using Omni glass columns, 6 cm in length, in place of the original experimental core. The pressure drop across the column was measured using a Validyne KP15 transducer. The column was filled with glass beads of various sizes. Foam was generated in the cell until the pressure drop across the column remained constant for a period of time, at which point steady state was reached. At this

point, the valves on the upstream and downstream sides of the cell were closed to isolate the foam inside. To present the data, time is zero when flow is stopped.

The experiment was done for three different size beads. The intermediate bead size was 160 μm. Figure 17 shows the behavior of the pressure drop across the column in this case. The initial negative slope of pressure drop as a function of time is very steep. Immediately upon isolating the foam in the system, hydrodynamic flow continues as the lamellae rearrange. The rearrangement happens as the driving force for foam flow is removed, accounting for the initial steep decline. Then the slope suddenly decreases and the pressure diminishes uniformly until equilibrium is reached. This lower slope represents the period when diffusion is the only mechanism by which the pressure drop relaxes.

After hydrodynamic flow comes to a stop, there is still a pressure drop which must relax by diffusion. The pressure drop that exists across the system during flow acts as a driving force for diffusion of gas between adjacent bubbles. The net diffusion of gas is from the upstream side of the column to the downstream side. The diffusion-dominated regime can be approximated as a lognormal dependence of pressure drop on time, and this is discussed in more detail later. As gas diffuses in the flow direction, the driving force for diffusion is reduced, and the pressure drop across the column approaches zero. Ultimately, an equilibrium lamella configuration is achieved. All the lamellae end up at pore throats, where they have no curvature and thus sustain no pressure drop. At this point, the gas pressure is everywhere uniform.

As explained above, we can tell a lot about trends and system behavior by comparing the pressure gradient development and evolution for systems with various bead sizes. Using the fixed length column eliminates some confusion because there are no pores containing foam outside of the measurement region. When the pressure drop is measured between two of the pressure taps in the original core, gas diffuses from upstream bubbles into the measurement region and diffuses out of the measurement

region into downstream bubbles. We do not know what effect this has on the behavior of the system. Figures 18 and 19 show the history of the pressure drop due to the presence of foam in the Omni column for beads which are larger and smaller than those in Figure 17, respectively. The beads used in generating the data of Figure 18 are 250 μm in diameter, and the ones used for generating Figure 19 are 45 μm in diameter.

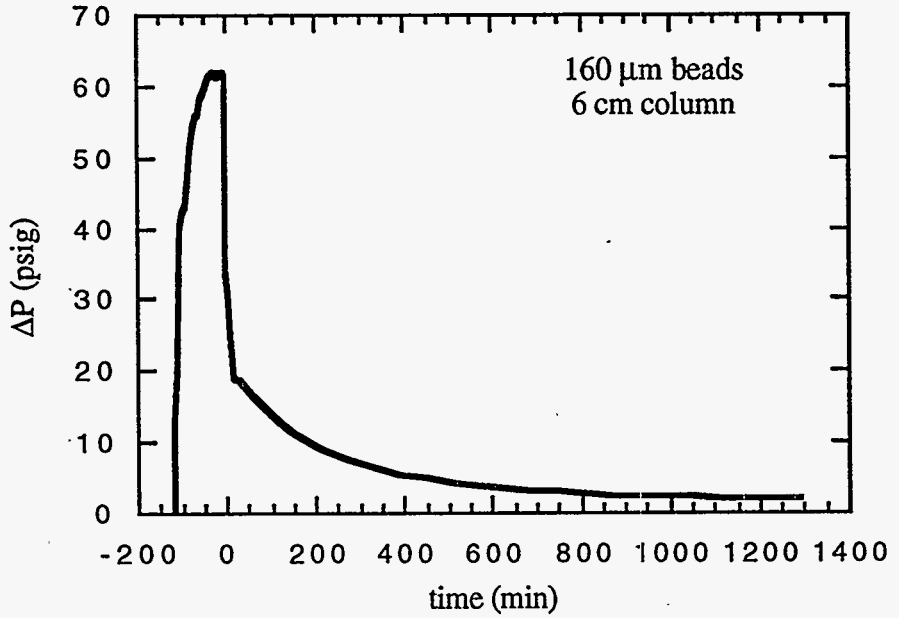

Figure 17: Evolution of pressure drop across the foam-filled column packed with 160 μm glass beads. Time zero corresponds to the isolation of foam in the column.

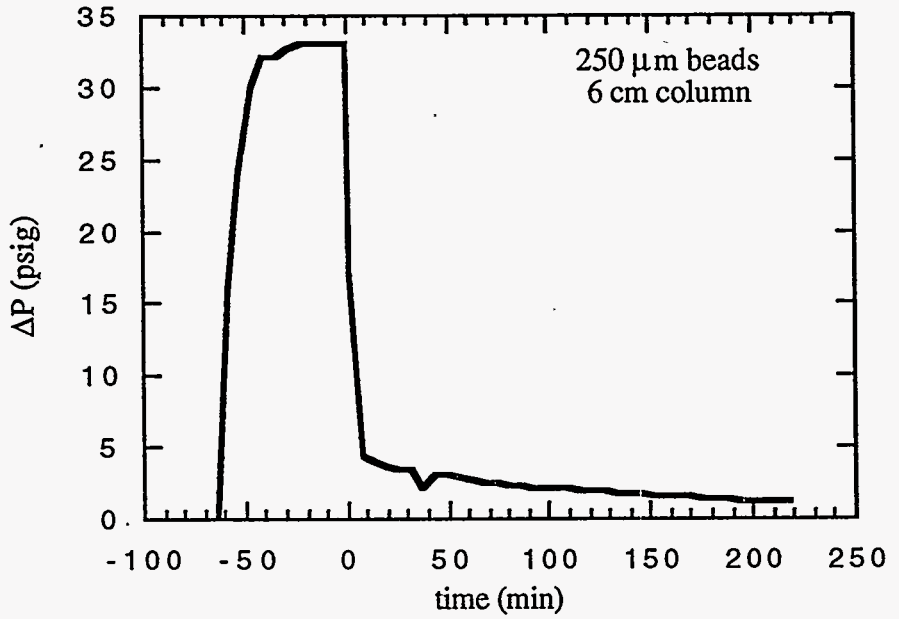

Figure 18: Evolution of pressure drop across the foam-filled column packed with 250 μm glass beads.

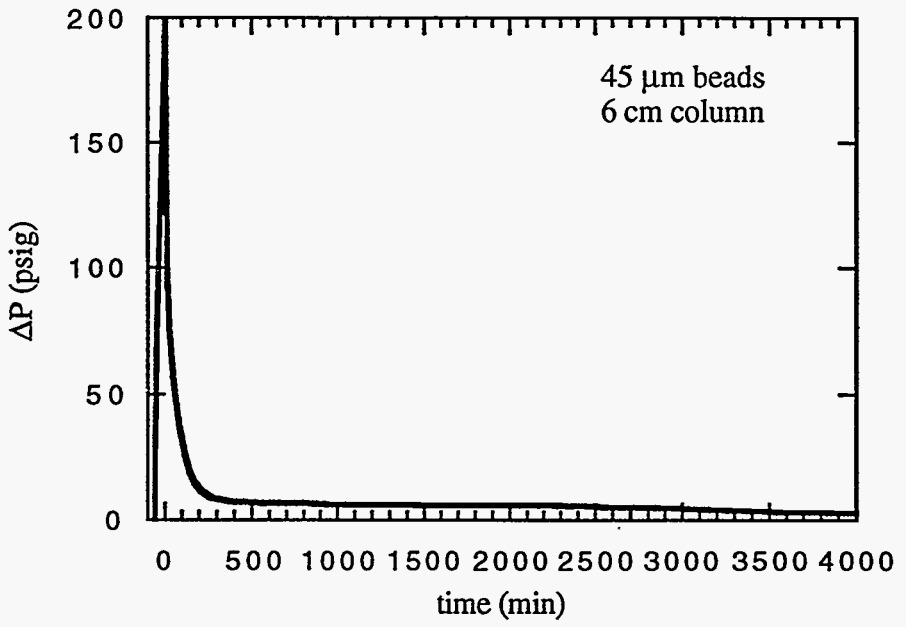

Figure 19: Evolution of pressure drop across the foam-filled column packed with 45 μm glass beads.

From the above figures, we see that the magnitude of the pressure drop at steady state foam flow is close to inversely proportional to bead size. In other words, when the core is packed with beads that are half the size, the pressure drop that exists upon completion of steady foam flow is twice as great. When the beads are half the size, twice the number of pores fill the space from one end of the core to the other. Since, on average, the foam texture is the same everywhere at steady state in a monodisperse bead pack, there are roughly twice the number of lamellae per unit length in the column when the beads are half the size. Since the pressure drop is twice as high for a system with twice the number of lamellae, the assertion can be made that each lamella in each system must on average sustain about the same pressure drop.

Pore geometry dictates that as a lamella gets closer to the pore throat, its radius of curvature increases, and thus the pressure drop it sustains is lower. But for smaller pores, the pressure drop that a lamella sustains at a given position is greater. So, in the system with smaller pores, the lamellae probably sit, on average, closer to the pore throats when

flow stops. A more detailed explanation of pore geometry and its effect on lamella characteristics can be found elsewhere.[10]

There are several mechanisms which may affect the rate of relaxation of pressure drop across a column containing foam in a porous medium. The first is system length, based on number of pores in the system. The more pores there are, the more lamellae there will be, and therefore the harder it is for the two ends of the column to communicate with one another. This would tend to cause the system to take longer to reach equilibrium. The second mechanism deals with the rate of diffusion. Based on the conclusion that the pressure drop across each lamella is approximately the same, the rate of diffusion across each is, on average, the same. However, because the lamellae in the smaller pores are closer to the pore throats, they will achieve positions of zero curvature sooner. This effect acts counter to the effect of system length.

Because the two effects on time to equilibrium oppose one another, it is often hard to predict how long it will take a particular system to reach equilibrium. For systems with the same lamella distribution, we would expect the time to equilibrium to scale with inverse permeability, because the characteristic time for diffusion is R^2/D, where D is the gas-liquid diffusivity. However, it is impossible to generate the same foam configuration in each experiment. Even for the same size beads, the pressure gradient at steady state and its evolution vary, so we know that the steady state configuration is different each time. In systems with smaller pores, the variation in the lamella configuration results in faster diffusion times. This is the opposite of the conjecture that time to equilibrium is inversely proportional to permeability. The characteristic time is discussed in detail elsewhere.[10]

Foam Drainage

When foam is generated in a porous medium, a large pressure difference is required in order to keep it flowing. When flow stops, the pressure difference approaches

zero as gas diffuses from the upstream to the downstream end. As a result of diffusion, the lamellae rearrange and some coarsening occurs. The gas that remains at equilibrium is at a high pressure, one that is about equal to the average value of the pressure profile that existed when flow was stopped. If the process of diffusion led to the complete decay of foam, so that no lamellae remained, then opening the outlet value would result in complete ejection of the fluids happening in a short period of time.

If, however, foam lamellae still are present upon opening of the outlet valve, flow driven by the pressure drop that is created by opening the valve would take a significant length of time to drain out of the cell. Experiments verify that the foam that remains in the column at equilibrium is still a strong foam. The way this is done is once again by tracking the evolution of the pressure drop across the column after the outlet valve is opened.

When the downstream valve is opened, there is a sudden rush of foam bubbles out of the cell, corresponding to convective flow of foam lamellae driven by the pressure drop across the cell. Looking at the foam provides verification that the foam still has a fine texture. The fact that foam immediately emerges from the cell is another verification of the fact that the equilibrium configuration after diffusion is complete is a stable foam. If the foam had in fact completely disappeared, what would emerge immediately out of the cell would be the individual phases, and not foam bubbles at the fine texture we observe. The pressure drop across the column would rapidly disappear, as the individual gas and liquid phases do not resist flow like foam does. The sudden motion of the two phases would cause some foam to form, but it would not have as fine a texture because it takes a longer period of time to achieve the equilibrium texture that we observe.

After the sudden rush of foam bubbles out of the cell, the foam takes a long time to equilibrate to atmospheric pressure. This is because foam lamellae decrease the gas mobility and thus limit the drainage out of the column to that caused by diffusion of gas, which is significantly slower than convective flow of foam or continuous gas phase. This

is verified by the fact that during the slow emptying of a foam-filled porous medium, no liquid is observed to exit from the column, even as the pressure drop across the column continues to decrease toward zero.

When the outlet valve is opened, the pressure drop across the column jumps up to a value equal to half the value of the pressure drop that existed when the original flow was stopped. Presented below are the drainage behaviors of two of the experiments presented in the previous section. Figure 20 shows the data for the 160 μm system. When the valve is opened (t=0), the pressure drop across the column jumps to 31.5, which is exactly half the value of the pressure at steady state in Figure 18.

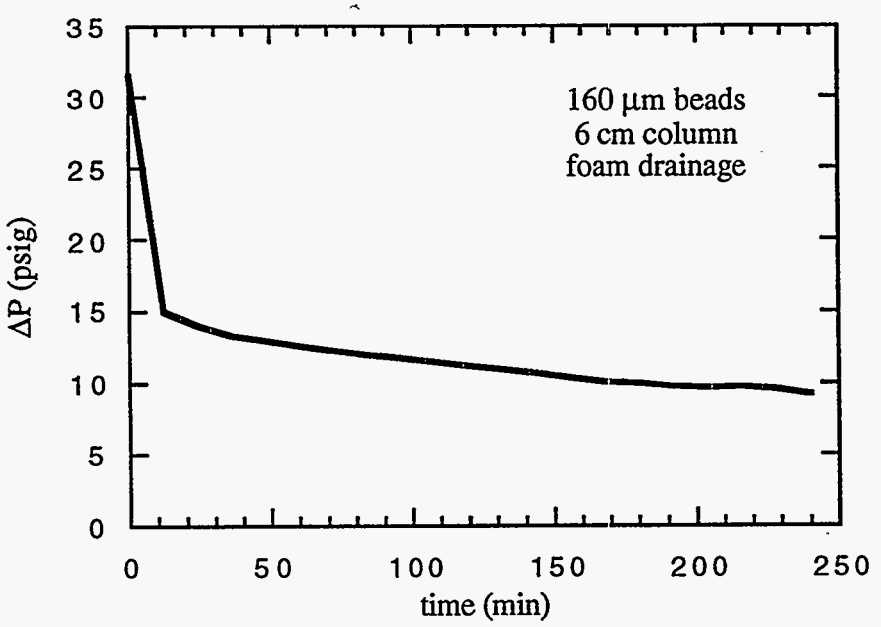

Figure 20: Drainage of foam out of a column packed with 160 μm beads.

The fact that the pressure drop immediately after the outlet valve is opened is half of the steady state flow pressure drop is an independent verification that steady state was achieved during foam generation. At steady state, the pressure profile along the length of the column is approximately linear. When the foam is isolated inside the column, the system rearranges by quick hydrodynamic motion followed by a long period of diffusive flow of gas. The result is a uniform pressure which has a value equal to the pressure at

the mid-point of the column at steady state flow conditions. This behavior is illustrated schematically in Figure 21. The pressure profile labeled #1 is the steady state pressure profile, at which time the inlet pressure is significantly higher than the outlet pressure. Pressure profile #2 is the uniform pressure that exists at equilibrium after gas diffusion is complete in foam that is isolated in a porous medium. When the outlet valve is opened, there is a large driving force for flow out of the column and very quickly a pressure gradient at the outlet (#3) must be formed which is greater than the mobilization pressure for foam of the existing texture in the porous medium. Predictions of the required mobilization pressure are described in Cohen's thesis.[3] As long as a large enough pressure gradient exists, hydrodynamic flow of foam out of the column continues until the pressure profile across the column takes the form of #4. At this point, there is not enough of a pressure gradient to cause flow of foam, and the foam remains trapped. This occurs for the system of Figure 20 at a pressure gradient of 17 atm/m, which corresponds to ΔP=15 psi for the 6 cm column. The time when trapping occurs is easily identified in Figure 20 as the time when the slope suddenly changes.

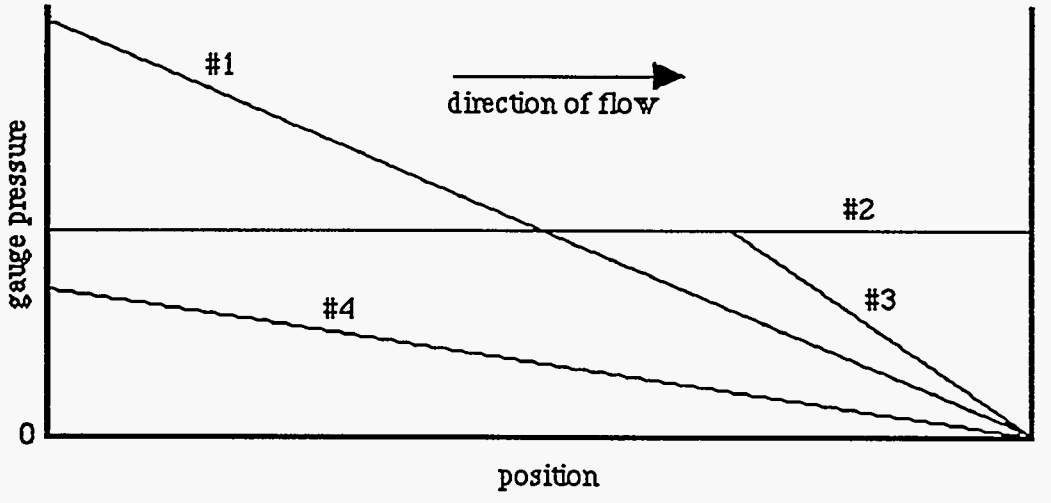

Figure 21: Schematic illustration of the pressure profile evolution of isolated foam and remobilized foam in a porous medium. At flow steady state, profile #1 exists. When flow is stopped, the profile evolves to the equilibrium profile (#2). When the outlet valve is opened, rapid flow of foam out of the medium is driven by profile #3. Eventually, hydrodynamic flow ceases because there is not enough driving force to move lamellae through the porous medium. This occurs when the profile #4 is reached. This profile serves as a driving force for gas diffusion.

Once hydrodynamic flow has stopped and foam is trapped in the porous medium under pressure profile #4 in Figure 21, the system continues to relax as gas diffuses through the lamellae from the high pressure side of the column out through the exit. This diffusion-driven drainage of foam lasts a very long time. The small slope at long times in Figures 20 and 22 indicates the slow rate of gas diffusion leading to complete loss of pressure in the column. Figure 22 shows the data for the drainage process in the case where the column is packed with 250 μm glass beads.

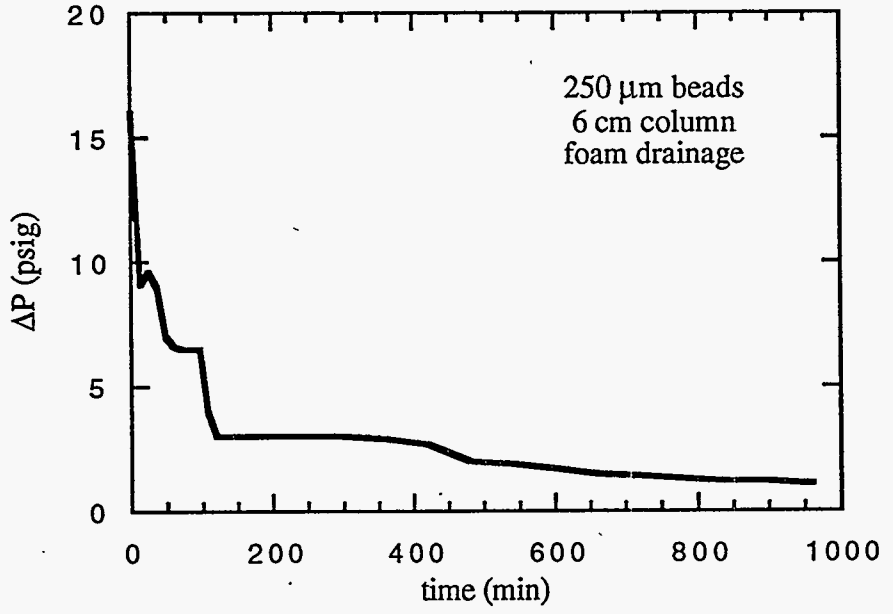

Figure 22: Drainage of foam out of a column packed with 250 μm beads.

Comparison of Experiments to Theory

We have presented experiments to illucidate the behavior of stationary foam in porous media. These include measurements of the change in pressure of a "headspace" adjacent to a porous medium, as well as the evolution of the pressure gradient initially created during propagation of foam through a porous medium. These experiments teach us how gas diffusion affects the behavior of stationary foam in porous media.

Novel computer simulations that predict the evolution of foam topology and pressures in porous media have been presented elsewhere. Cohen *et al.* uncovers interesting behaviors that result from diffusion of gas in stationary foams that are under zero net imposed pressure gradient.[10] These simulations reveal the time dependence of the cooperative diffusion process and the complicated motion of individual lamellae. The paper describes some of the monumental challenges that arise in creating a mathematical description of foam in porous media. Nonlinearities and singularities result in multivalued solutions, that represent sudden rearrangements of lamellae in regions of the porous medium.

Chapter 4 of Cohen's thesis contains information about simulations that predict the behavior of foam in a porous medium that is under the influence of a net pressure gradient.[3] If the pressure gradient remains constant, gas continues to flow through the system by diffusion even when the foam is stationary. If the pressure gradient is below a certain mobilization pressure, the foam remains stationary indefinitely. If the mobilization pressure is exceeded, hydrodynamic flow eventually resumes, after some amount of coarsening of the foam texture. Knowledge of these trends allows us to predict the amount of foam that traps in a porous medium at a given pressure gradient. Trapping is predicted using a simple expression that can aid in the modeling of foam flow in porous media with a lognormal pore size distribution. The analytic expression accounts for the amount of foam mobilized at a given pressure gradient.

While most of the experimental results do not give us data which can be directly verified by the simulations, some of the trends and orders of magnitude can be compared with simulation results to ensure that the simulations reflect reality. In what follows, comparisons are made between time scales and pressure magnitudes found experimentally and scaling found from the simulations.

Two distinct regimes were observed in the experimental pressure drop decay process. Immediately after isolating flowing foam in the core, flow by convection

continues until the pressure gradient falls below the mobilization pressure drop for the system. At this point, diffusion takes over as the mechanism for loss of the pressure drop. This process is much slower, and thus it takes a very long time for the system to reach equilibrium. The diffusion regime seems to follow a lognormal behavior in time. Figure 23 shows the decay of the pressure drop in a 160 μm beadpack, the same results as given in Figure 17. Recall that the original build up of pressure occurs as flow results in foam generation in the porous medium. When foam reaches steady state, i.e., when the pressure drop levels off, flow into the core is cut off and there is an early time rapid relaxation of the pressure gradient as hydrodynamic flow settles. After this, the diffusion-driven regime takes over.

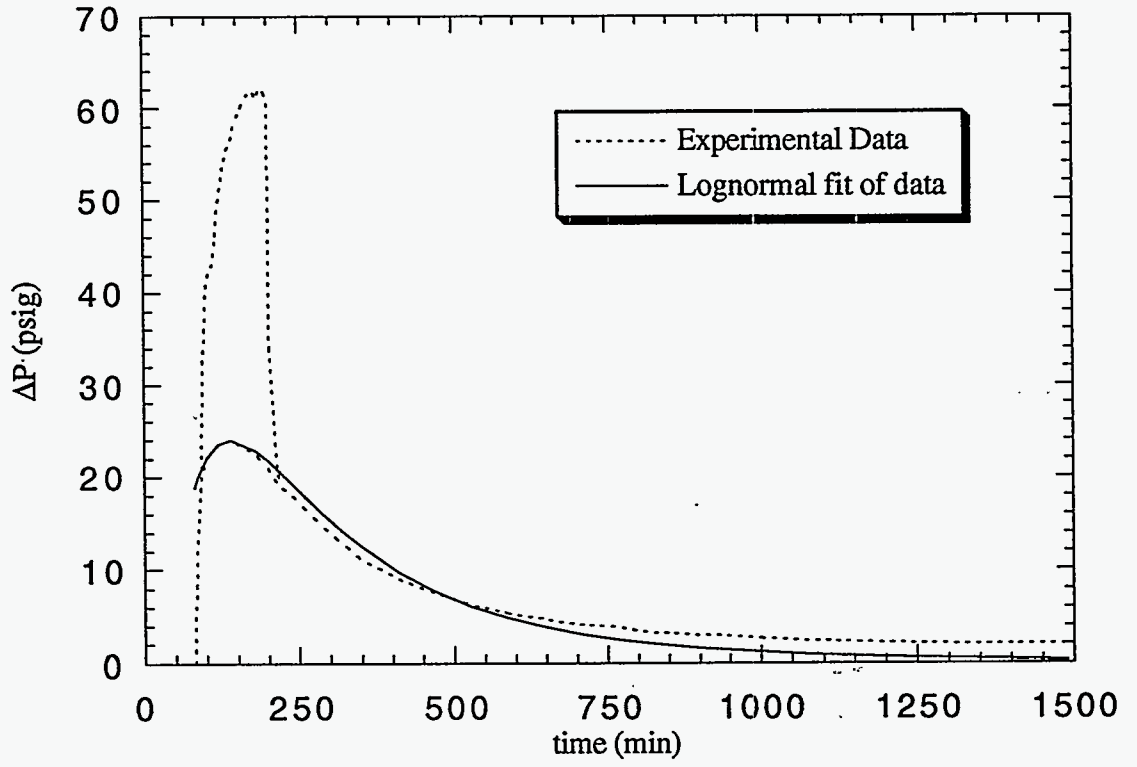

Figure 23: Evolution of the pressure drop across a foam-filled 6 cm core filled with 160 μm glass beads. The data are the dotted line. There are two distinct regimes. The second regime is completely diffusion driven, and has been extrapolated back to time zero in the figure. The solid line represents a lognormal fit of the diffusion driven regime.

In the presentation of the data in Figure 23, the diffusion regime is extrapolated back to time zero. In addition, a lognormal fit of the curve is shown in the figure. The lognormal scaling is fit using

$$\Delta P = b \exp\left[\frac{-(\ln t - \ln a)^2}{2s^2}\right], \qquad [3]$$

where a is the location of the peak in the extrapolated curve, b is the height of the peak, and s is the standard deviation of the curve.

Above, we compared the pressure drop relaxation for systems with various bead sizes. The same three sets of data are shown in Figure 24 along with the corresponding lognormal fit of the diffusion-controlled regime. As the bead size increases, the height of the peak in pressure drop decreases. Also, larger beads result in a broader lognormal shape, as evidenced by the increasing value of the standard deviation, s. The best fit of the data using Eq. [3] results in values of the parameter b of 100, 24, and 7.5 for the three bead sizes.

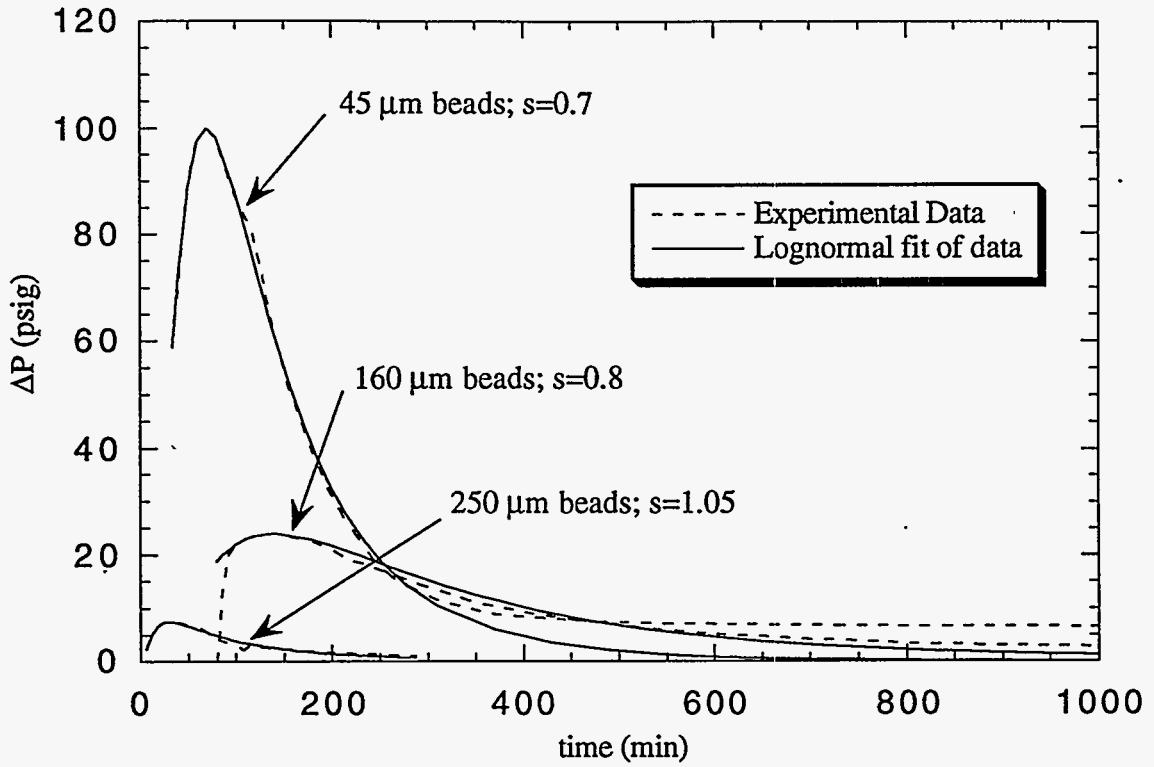

Figure 24: Plot of the diffusion-driven regime of the relaxation of the pressure drop across a 6 cm core filled with beads of varying sizes. The best fit using the lognormal distribution of Eq. [3] are shown.

The left end of the projection of the pressure drop curve represents an artificial creation of lamellae in a somewhat random configuration in order to allow the system to satisfy an initial pressure drop. Starting with this configuration, the pressure drop across the system increases before decreasing again, simply as a result of diffusion. This behavior is in fact predicted by the network simulations. The initial conditions used in a simulation tracking the evolution of the pressure gradient represent the artificial conditions described here. When we run a simulation from this set of initial conditions, the pressure drop across the system increases before decreasing again. Once again, these theoretical calculations, as shown in Figure 25 for three sets of conditions, can be fit by the lognormal expression [3].

The plot in Figure 25 shows dimensionless pressure drop as a function of dimensionless time. The nondimensionalization used is described in detail in Cohen's

thesis.[3] The pressure drop in these simulations is defined as the difference between the average gas pressure in all the upstream pore bodies and the average gas pressure in all the downstream pore bodies. Each system is the same length dimensional length. Thus, the smallest beads are used in a 20×3 network, while beads which are twice as large are used in a 10×3 network, etc. The initial dimensionless pressure drops are all the same. Since pressure is nondimensionalized by surface tension over the characteristic length (R), the initial dimensional pressure drop across the system is inversely proportional to the bead size.

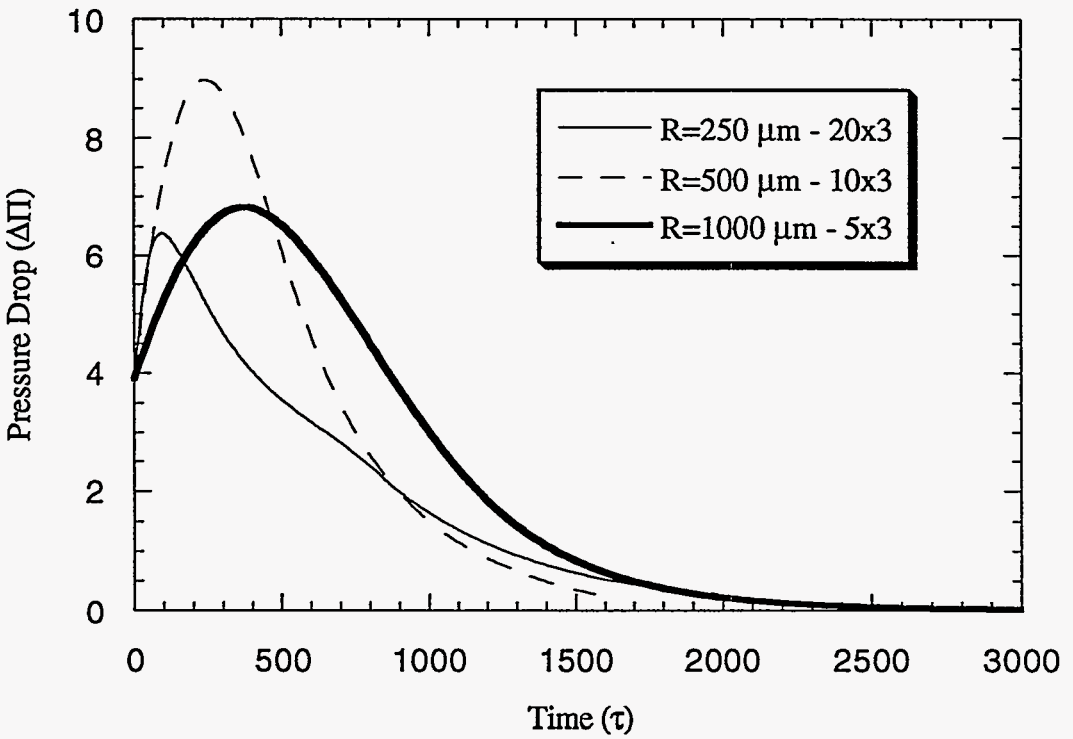

Figure 25: Calculated pressure drop as a function of time for different size beads and different size networks, which are all the same dimensional length. The initial dimensionless pressure drops are the same, and the pressure drop evolves in lognormal manner.

The characteristic time for the problem is defined in detail in the paper by Cohen *et al.*[3] In addition to the square of the characteristic length over the diffusivity, the time to reach equilibrium is also proportional to a constant, β, which defines the ease of

transport of the gas through the liquid and the characteristic pressure. The characteristic pressure is inversely proportional to the square of the characteristic length and β is inversely proportional to the characteristic length. Overall, dimensional time is proportional to the characteristic length.

While the results shown in Figure 25 reproduce the shape of the diffusion regime of the pressure gradient relaxation, they do not accurately predict the time scale over which the pressure drop disappears. The network simulation shows dimensionless times to reach equilibrium that are equal for systems with different grain sizes. Using the characteristic time, this corresponds to longer times for systems with larger characteristic lengths. However, the experiments have shown the opposite result: systems made up of smaller beads take longer to reach equilibrium.

A probable reason for this discrepancy is that the simulations only are done for relatively small networks. The conditions used are those which would occur near the exit. Over the full length of a core, the pressure drop becomes significant. Therefore, the average gas pressure is much higher in systems with smaller beads than in systems with larger beads, even though the initial downstream pressures are the same. The time to equilibrium is linearly proportional to the system pressure.[3] So the systems with smaller beads, which have a significantly higher pressure, would slow down simply due to the fact that there is more gas which must rearrange before equilibrium is achieved.

We conclude that the simulator describes the diffusion dominant regime of pressure gradient relaxation in foam which is isolated in a porous medium. But the simulator cannot be used to model the actual pressure gradient behavior, because the actual behavior is a reflection of the sheer magnitude of a porous medium, i.e. the tremendous number of pores that make up a porous medium. Due to the computational force required to solve the equations involved, our simulator is limited to smaller networks, which cannot capture the essence of very large ones.

Experiments tracking the change in headspace pressure both above a bulk foam and alongside foam in a porous medium are presented earlier in this paper. The typical experiment done with 1 mm glass beads results in a gas pressure increase of about 0.1 psi over a time period of about 150 minutes. These are very small pressure increases, that are extremely difficult to measure accurately.

The simulations give order of magnitude behavior which can be compared with the experimental results.[3] The simulation provides the evolution of all the gas bubble pressures as a function of time. The result of the simulation which interests us is the increase in pressure of one pore body. This is not strictly the same thing as the increasing pressure in the large artificial headspace, but can shed light on whether or not the simulation and experiment relate to one another. The headspace in the experiment is basically a very large pore body with a high coordination number. Rather than having four pores surrounding the pore body, this "body" has hundreds. Therefore, the ratio of pore volume surrounding the body to the volume of the body itself is comparable.

For comparison purposes, we run a 3×3 simulation as described using a characteristic grain size of 500 μm (0.5 mm). The resulting dimensionless pressure increase in the first pore body is 1.3. This converts to a pressure increase of 0.013 psi. This is the same order of magnitude as the 0.06 psi pressure increase found experimentally. The simulation gives a time to equilibrium of 130 minutes. This again is similar to the equilibrium time of 160 minutes in the experiment of Figure 14. Even though the two systems might not be fully comparable, the fact that they both settle to equilibrium in the same amount of time helps us feel more comfortable about using the simulation to predict the behavior of real systems. In fact, the agreement is quite good considering that the pressure increase cited from the simulation is the increase in pressure at an individual pore body, whereas the pressure increase in the experiment is that of the entire headspace adjacent to the porous medium.

Chapter 4 of Cohen's thesis describes the pressure drops required to mobilize foam through a porous medium.[10] The calculation is done assuming the texture of the foam is such that there is one lamella residing in each pore throat. Our experiment's showed huge pressure drops which were required to keep foam flowing through a porous medium during the generation process. The pre-equilibrium pressure drop of 210 psi across the 6 cm core filled with 45 μm beads in Figure 19 is equivalent to 240 atm/m. With one lamella per pore, the simulation gives a mobilization pressure gradient of 450 atm/m.

There is even better agreement for systems with larger pores. For 160 mm beads, the calculated mobilization pressure, for one lamella per pore, is 40.7 atm/m. The experimental pressure drop at flow equilibrium in Figure 17 translates to a pressure gradient of 70 atm/m. When the foam is isolated and coalescence is complete, the pressure gradient sustained by the porous medium when the outlet valve is opened is 35 atm/m. This is very close to the calculated mobilization pressure gradient.

The discrepancy between the predicted mobilization pressure gradient and the experimental value may be caused by a couple of things. First, the quality of packing of the glass beads varies from system to system. The predicted mobilization pressure gradient is calculated assuming that each pore body is the same size as the pore next to it. If, in fact, the pore bodies are a bit longer, the required pressure gradient is lower because there are fewer lamellae to be mobilized in a given length. In addition, all the calculations are done assuming a texture such that there is one lamella per pore in the system. This is the maximum texture that can exist. However, this texture may not be realized in a real system. Fewer lamellae in the system than the maximum texture allows explains the fact that our predicted values of mobilization pressure are higher than the experimental values. The discrepancy is usually less than a factor of two, so the actual foam texture falls somewhere between one lamella every one and a half pores.

Summary

Experiments have been performed to understand the behavior of foam isolated in a porous medium. A core was designed which allows in situ generation of foam and has pressure taps along the side. At these pressure taps, semi-permeable membranes can be used to separate the phases. The idea is to create a large gas bubble adjacent to the porous medium which is analogous to the headspace above a bulk foam. Attempts were made to measure the change of pressure in this "headspace" for various size bead packs. The measurement is only possible for the largest bead size, with 1 mm diameter. Any bead size below this results in a pressure drop across the column which is too high. The adjustment of this pressure drop overpowers any increase in headspace pressure.

The results for the 1 mm diameter bead pack are presented. The increase in pressure is very small, but does verify the assertion that gas is released from the pore throats into the pore bodies as a result of gas diffusion. The core was used also to reproduce the data of Monsalve and Schechter[10] for increase in headspace pressure above a decaying bulk foam.

Since the pressure difference across the core filled with isolated foam is significant and eventually disappears as the system approaches equilibrium, it is very informative to track this pressure difference as a function of time. The data show that smaller bead packs result in a higher pressure difference and a longer time to reach equilibrium. The scaling is not so simple because the distribution of lamellae is not the same for different size bead packs. The difference in lamella distribution causes the system to take less time to decay than expected for lower permeability bead packs.

As foam generates and propagates in a porous medium, it moves through the core as a uniform front. The motion of the front is presented with a series of snapshots of the core during foam generation and propagation. The pressure drop across the column builds up until steady state is reached, at which point the pressure drop is linear for incompressible fluids. Experiments can be done to verify that the pressure drop was in

fact linear at the point where flow is stopped. These same experiments tell us that a strong foam remains in the column even long after foam flow has ceased. Therefore, diffusion does not result in the complete destruction of foam, rather it results in an equilibrium foam which is still strong and resists flow.

There are two regimes for the evolution of pressure gradients in foam. These have been observed in stationary foam in a porous medium and also as foam is allowed to flow out of the porous medium. The first regime is one where the mobilization pressure is exceeded and foam lamellae flow by hydrodynamic motion. The second regime occurs when the mobilization pressure is no longer exceeded and diffusion is the only mechanism by which the pressure gradient relaxes. The division between the two regimes is indicated by a sudden change in slope on a plot of pressure difference versus time.

Certain elements of the experiments and simulations can be compared with one another in order to help verify the existence of certain mechanisms. Different simulations are invoked in comparison with the various experiments performed. First, an in-depth look is taken at the evolution of the pressure gradients. We recognize that the diffusion regime in the relaxation, when projected back to time zero, follows a lognormal shape. The simulations start with a somewhat random initial configuration of lamellae and result in a lognormal shape as well. Even though the simulations do not quantitatively predict the experimental results, the qualitative match is striking.

The increasing pressure in a gas bubble adjacent to the porous medium is expected because the gas bubble acts as a large pore body connected to many individual pores. The bubbles in the individual pores trap gas inside, and this gas slowly seeps out of the pores by diffusion and ends up in the larger bubble. The magnitude of the pressure increase and the length of time to equilibrium matches within an order of magnitude to that predicted by the model simulations.

The last model predicts the magnitude of the mobilization pressure gradients required to keep foam flowing through a porous medium. These magnitudes match very closely with the pressure drop which develops when foam is allowed to flow out of a core after reaching diffusion equilibrium. Therefore, the large magnitudes predicted to be needed to mobilize foam are realistic in systems with finely textured foams. The foams in our experiments have fine textures, made so by flow rates that are actually somewhat larger than those which are used in most field applications.

Nomenclature

a - location of the peak in diffusion-driven pressure drop relaxation (min)

b - peak height in lognormal fit of pressure drop relaxation data (psi)

Bo - Bond number

c - constant for finding permeability from bead diameter in packed bed

D - diffusivity of gas through liquid phase (m^2 / s)

g - gravitational acceleration (m/s^2)

h - height (m)

K - permeability (m^2)

ΔP - pressure drop (psi)

r - pore throat radius (m)

R - diameter of beads in packed core (m)

s - standard deviation in lognormal fit of pressure drop relaxation data (min)

t - time (min)

ρ - density (kg/m^3)

σ - liquid/gas interfacial tension (N/m)

$\Delta\Pi$ - dimensionless pressure drop

τ - dimensionless time

References

1. Nishioka, G., S. Ross and M. Whitworth "The stability of foam: Comparison of experimental data and computed results," *J. Coll. Interf. Sci.* 1983 *95(2)*, 435-442.

2. Ross, S. "Bubbles and foam: New general law," *Ind. Eng. Chem.* 1969 *61(10)*, 48-57.

3. Cohen, D. PhD Thesis, University of California at Berkeley, 1996.

4. Flumerfelt, R. W., H.-L. Chen, M.-J. Ke and T.-K. Chuang "Experimental studies of capillary pressure effects of foams in porous media," SPE 20069, Presented at 60th California Regional Meeting, Ventura, CA, Apr. 4-6, 1990.

5. Chambers, K. T. and C. J. Radke "Capillary Phenomena in Foam Flow Through Porous Media," *Interfacial Phenomena in Petroleum Recovery*, New York: Marcel Dekker, Inc., 1990.

6. Kovscek, A. R. and C. J. Radke "Fundamentals of Foam Transport in Porous Media," *Foams: Fundamentals and Applications in the Petroleum Industry*; Advances in Chemistry Series 242, ed. Laurier L. Schramm, Chapter 3, 1994, 113-163.

7. Rossen, W. R. "Theory of mobilization pressure gradient of flowing foams in porous media (parts i, ii, iii, iv)," *J. Coll. Interf. Sci.* 1990 *136(1).*

8. Hanssen, J. E. and P. Haugum "Gas blockage by non-aqueous foams," SPE 21002, Presented at SPE International Symposium on Oil-Field Chemistry, Anaheim, CA, 1991.

9. Fagan, M. MS Thesis, University of California at Berkeley, 1992.

10. Cohen, D., T. W. Patzek and C. J. Radke "Two-Dimensional Network Simulation of Diffusion Driven Coarsening of Foam Inside a Porous Medium," *J. Coll. Interf. Sci.* 1996 *179*, 257-373.

11. Nishioka, G. and S. Ross "A New Method and Apparatus for Measuring Foam Stability," *J. Coll. Interf. Sci.* 1981 *81(1)*, 1-7.

12. Schechter, R. S. and A. Monsalve "The stability of foams: dependence of observation of the bubble size distribution," *J. Coll. Interf. Sci.* 1984 *97(2)*, 327-335.

13. Hubbert, M. K. "Darcy's Law and the Field Equations of the Flow of Underground Fluids," *J. Petr. Technol.* 1956 *8(10)*, 222-239.

14. Mast, R. F. "Microscopic Behaviour of Foam in Porous Media," SPE 3997, Presented at 47th SPE Annual Mtg., San Antonio, TX, October, 1972.

15. Ransahoff, T. C. and C. J. Radke "Mechanisms of Foam Generation in Glass-Bead Packs," *SPE Res. Eng.* May 1988, 573-585.

16. Schramm, L. L. *Foams: Fundamentals and Applications in the Petroleum Industry*; Washington, DC: American Chemical Society, 1994.

17. Patzek, T. W. "Self-Similar Collapse of Stationary Bulk Foams," *AIChE J.* 1993 *39(10)*, 1697-1707.

18. Lin, C. Y. and J. C. Slattery "Three-Dimensional, Randomized, Network Model for Two-Phase Flow Through Porous Media," *AIChE J.* 1982 *28(2)*, 311-324.

19. Bikerman, J. J. *Foams*; Berlin: Springer-Verlag, 1973.

☆U.S. GOVERNMENT PRINTING OFFICE: 1996 - 760-032/40025